Spatial Prediction of Groundwater Spring Potential Mapping Based on Adaptive Neuro-Fuzzy Inference System and Metaheuristic Optimization

Khabat Khosravi[1], Mahdi Panahi*[2], Dieu Tien Bui*[3]

1-Department of watershed management engineering, Faculty of Natural Resources, Sari Agricultural Science and Natural Resources University, Sari, Iran. (E-mail: khabat.khosravi@gmail.com)

2- Department of Geophysics, Young Researchers and Elites Club, North Tehran Branch, Islamic Azad University, Tehran, Iran. (E-mail: panahi2012@yahoo.com)

3- GIS group, Department of Business and IT, University of South-Eastern Norway, Gullbringvegen 36, 3800 Bø i Telemark, Norway. (E-mail: Dieu.T.Bui@usn.no)

Abstract

Groundwater is one of the most valuable natural resources in the world; however, the groundwater is not an unlimited resource, therefore understanding groundwater potential is crucial to ensure its sustainable use. The aim of the current study is to propose and verify new artificial intelligence methods for spatial prediction of groundwater spring potential mapping at the Koohdasht-Nourabad plain, Lorestan province, Iran. These methods are new hybrids of Adaptive Neuro-Fuzzy Inference System (ANFIS) and five meta-heuristic algorithms, namely Invasive Weed Optimization (IWO), Differential Evolution (DE), Firefly Algorithm (FA), Particle Swarm Optimization (PSO), and Bees Algorithm (BA). A total of 2463 spring locations were identified and collected, and then, divided in two subsets randomly: 70% (1725 locations) were used for training models and the remaining (30%, 738 spring locations) were utilized for evaluating the models. Thirteen groundwater conditioning factors were prepared for modeling, namely slope degree, slope aspect, altitude, plan curvature, stream power index (SPI), topographic wetness index (TWI), terrain roughness index (TRI), distance from fault, distance from river, land-use/land-cover, rainfall, soil order, and lithology. In the next step, the Stepwise Assessment Ratio Analysis (SWARA) method was applied to quantify the degree of relevance of these groundwater conditioning factors. The global performance of these derived models was assessed using the Area Under the Curve (AUC). In addition, the Friedman and Wilcoxon signed rank tests were carried out to check and confirm the best model to use in this study. The result showed that all models have high prediction performance; however, the ANFIS-DE model has the highest prediction capability (AUC = 0.875), followed by the ANFIS-IWO model, the ANFIS-FA model (0.873), the ANFIS-PSO model (0.865), and the ANFIS-BA model (0.839). The results of this research can be useful for decision makers responsible for sustainable management of groundwater resources.

Keywords: Groundwater spring, ANFIS-DE, ANFIS-IWO, ANFIS-FA, ANFIS-PSO, ANFIS-BA, Iran.

1. Introduction

Groundwater is defined as the water in a saturated zone which fills rock and pore spaces (Berhanu et al., 2014; Fitts, 2002), whereas groundwater potential is the probability of groundwater occurrence in an area (Jha et al., 2010). The occurrence and movement of groundwater in an aquifer are affected by various geo-environmental factors including lithology, topography, geology, fault and fracture and its connectivity, drainage pattern, and land-use/land-cover (Mukherjee, 1996). Geological strata acts like a conduit and reservoir for groundwater while storage and transmissivity influence the suitability of exploitation of groundwater in a given geological formation. Downhill and depression slopes impart runoff and improve recharge and infiltration, respectively (Waikar and Nilawar, 2014). Globally, groundwater is a major source of drinking water for around two billion people(Richey et al., 2015), whereas in agriculture, about 278.8 million ha of agricultural lands are irrigated by the groundwater (Siebert et al., 2013). Due to population and economic growth, the demand of groundwater is anticipated increasing in the future (Ercin and Hoekstra, 2014). For the case of Iran, approximately two-third of the land is covered by deserts and groundwater is still the main water source for drinking and other uses (Nosrati and Van Den Eeckhaut, 2012). According to Rahmati et al. (2016), groundwater in Iran supplies around 65% of the water use-up and the remaining 35% is supplied by surface water. However, groundwater is not an unlimited resource, therefore understanding groundwater potential is crucial to ensure its sustainable use. One of the most efficient methods for the protection and management of groundwater to identify groundwater potential zoning (Ozdemir, 2011b).

There are a number of methods for groundwater potential zoning and exploitation. Traditional methods i.e. drilling, geological, geophysical, and hydrogeological methods are the most widely used (Israil et al., 2006; Jha et al., 2010; David Keith Todd and Mays, 1980; Sander et al., 1996; Singh and Prakash, 2002). However, they are time-consuming and costly methods, especially for large areas. In recent years, Geographic Information Systems (GIS) and remote sensing (RS) have become effective tools for groundwater potential mapping (Fashae et al., 2014) due to their ability in handling huge amount of spatial data.

In more recent years, some probabilistic models such as frequency ratio (Oh et al., 2011), multi-criteria decision analysis (Kaliraj et al., 2014; Rahmati et al., 2015), weights-of-evidence (WoE) (Pourtaghi and Pourghasemi, 2014), logistic regression (Ozdemir, 2011a; Pourtaghi and Pourghasemi, 2014), evidential belief function (Nampak et al., 2014; Pourghasemi and Beheshtirad, 2015), and Shannon's entropy (Naghibi et al., 2015) have been considered for groundwater potential mapping. Bivariate and multivariate statistical models have disadvantages in measuring the relationship between groundwater occurrence and conditioning factors (Tehrany et al., 2013; Umar et al., 2014), whereas MCDA technique is a source of bias due to expert opinion. Therefore, machine learning has been considered and has proven efficient due to ability to handle non-linear structured data from various sources with different scales. In addition, machine learning requires no statistical assumptions. Among machine learning methods, artificial neural network (ANN) is a widely used method for groundwater mapping due to its computational efficiency (Sun et al., 2016; Mohanty et al., 2015; Maiti and Tiwari, 2014). However, the ANN model has a number of weaknesses such as poor prediction and error in modeling process (Bui et al., 2016); therefore, hybrid models have been proposed. Among hybrid frameworks, ensemble of fuzzy logic and neural networks i.e. Adaptive Neuro-Fuzzy

Inference System (ANFIS) has proven it's efficient in term of high accuracy (Lohani et al., 2012; Emamgholizadeh et al., 2014; Zare and Koch, 2018; Nourani et al., 2016). It should be noted that although ANFIS model has a higher accuracy than other models, it is still difficult in finding the best internal weight values of ANFIS due to the limited nature of the adaptive algorithm used (Bui et al., 2016). Thus, these weights should be optimized by new metaheuristic optimization algorithms to enhance the prediction accuracy of ground water models.

The main goal of the current study is to propose and verify integration of new metaheuristic optimization algorithms with ANFIS for groundwater spring potential mapping (GSPM) in Koohdasht-Nourabad plain, Iran. Accordingly, five new metaheuristic algorithms are investigated, Invasive Weed Optimization (IWO), Differential Evolution (DE), Firefly Algorithm (FA), Particle Swarm Optimization (PSO), and Bees algorithm (BA). According to current literature, it is the first time such study is conducted for groundwater potential mapping.

2. Description of the study area

Koohdasht-Nourabad plain is located in the western part of the Lorestan province (Iran) and covers an area of around 9531.9 km^2. It lies between latitudes 33°3′ 28 N and 34° 22′ 55 N, and between longitudes 46° 50′ 19 E and 48° 21′ 18 E (Figure 1). The region is located in the semi-arid area with mean annual precipitation of about 450 mm (Iran Meteorological Organization). The altitude of the study area varies between 531 m and 3175 m above sea level. The maximum slope and minimum slope are 64^o and 0^o, respectively. Geologically, the study area is located in the Zagros structural zone of Iran and is mostly covered by Quaternary and Cretaceous-Paleocene geologic time scale. The dominant land-use/land-cover of the study area is moderate forest (20%). The residential areas cover about 3% of the plain. Rock crop/inceptisoils are the dominant soil types in the study area and covering about 51% of the study area. Population of the plain is 362,000 people (according to 2016 census) and agriculture is the primary occupation. In this plain, groundwater is the main water source for drinking and agricultural activities.

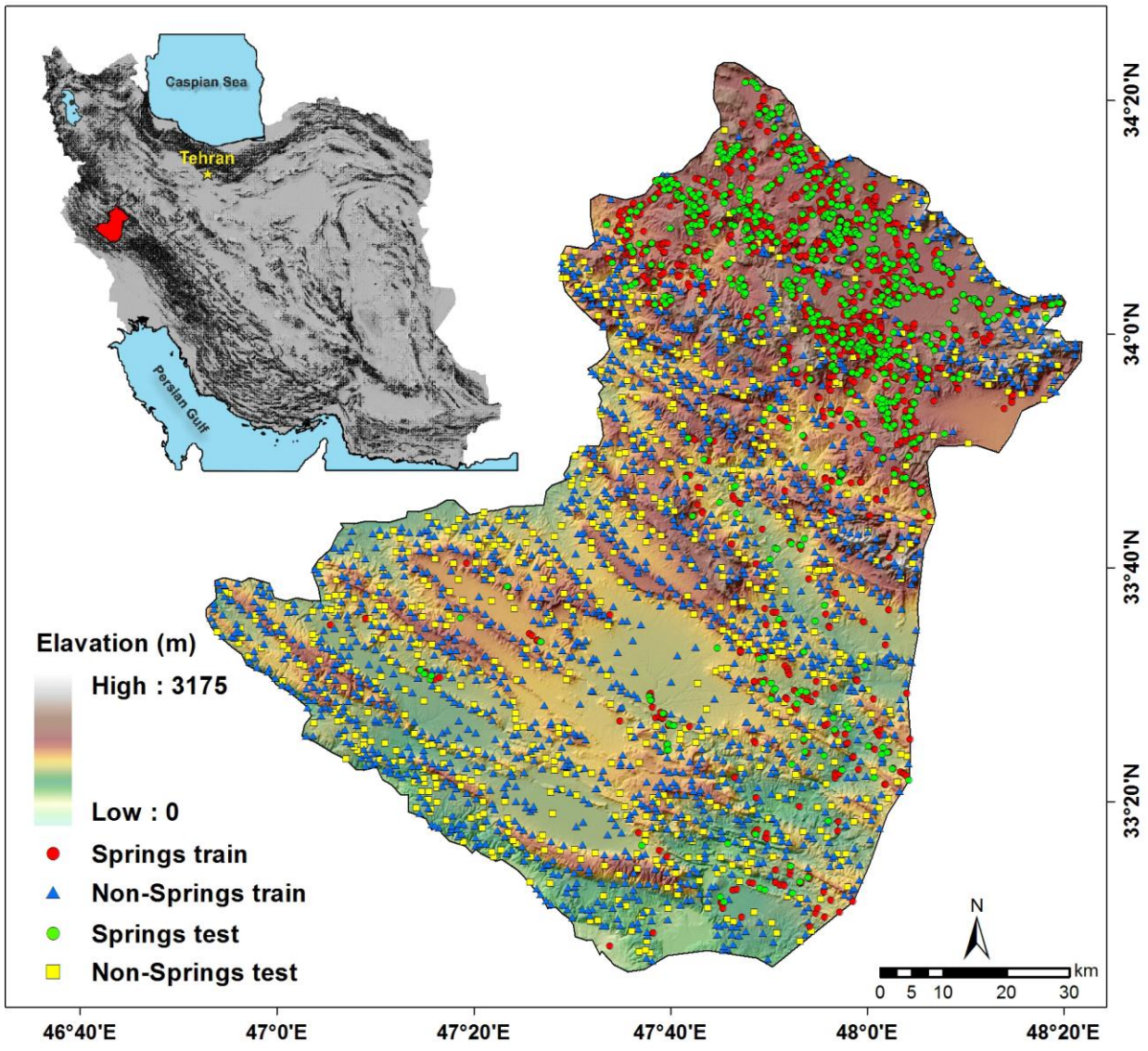

Figure 1. Groundwater well locations with DEM of the study area.

3. Methodology

An overview of the methodological approach is shown in Fig 2.

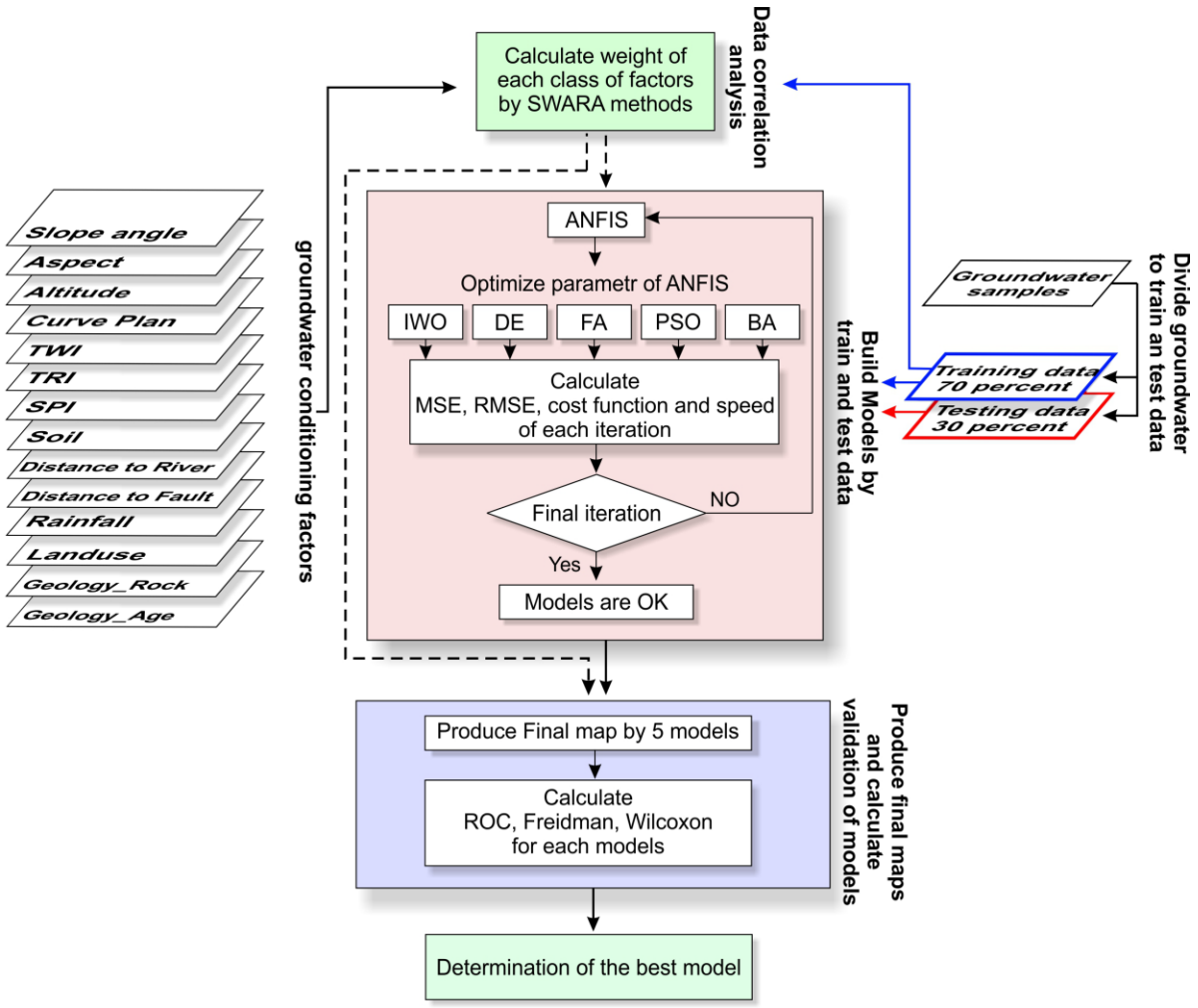

Figure 2. Conceptual model of methodology applied in the current study.

3.1. Data preparation

3.1.1. Groundwater spring inventory map

In groundwater modeling, spatial relationships between groundwater springs and conditioning factors should be analyzed and assessed to determine the best subset of these factors. In the Koohdasht-Nourabad plain, a total of 2463 spring locations were provided by Iranian Water Resources Management Bureau. Most of these spring locations were checked during extensive field surveys using a GPS hand held unit.

3.1.2. Construction of the training and testing datasets

Spatial prediction of groundwater potential mapping using machine learning model is considered a binary classification with two classes, spring and non-spring. Therefore, a total of 2463 non-spring locations were randomly generated using the random point tool in ArcGIS10.2. According to Chung and Fabbri (2003), it is possible to validate the model performance using a cross validation method that splits the dataset into the two parts for both of spring and non-spring location. The first part is used for model building which is called a training dataset and the other

part is utilized for validating the model performance named as a testing dataset (Pham et al., 2017a). In this study, a ratio of 70/30 was selected randomly for generating the training and testing the dataset (Pourghasemi et al., 2012; Pourghasemi et al., 2013a; Pourghasemi et al., 2013b; Xu et al., 2012). Accordingly, both spring locations and non-spring locations have been randomly divided into two groups for training (1725 locations) and validating (738 locations) purposes (Figure 1).

Both the training and the testing datasets were converted to raster format where spring pixels were assigned as "1" and non-spring pixels were assigned to "0" (Bui et al., 2015), and then, these pixels were overlaid with 13 groundwater conditioning factors to extract their attribute values.

3.1.3. Groundwater conditioning factor analysis

3.1.3.1. Selection of the Groundwater conditioning factor

After the initial selection of the conditioning factors, these factors should be assessed for multi-collinearity problems. Multi-collinearity takes place when two or more independent conditioning factors are highly correlated or in other words inter-dependent (Li et al., 2010). Several methods have been proposed to diagnose multi-collinearity, and among them, Variance Inflation Factor (VIF) and Tolerance (TOL) are widely used in environmental modeling (O'brien, 2007; Bui et al., 2016); therefore, they were selected for this research. Factors with VIFs greater than 5 and TOL are less than 0.1 indicate multi-collinearity problems existed (O'brien, 2007; Bui et al., 2011). Another method namely Information Gain Ratio (IGR) technique was applied to identifying the relative importance of the conditioning factor and also to obtain factors with null effect. These factors must be removed to increase the accuracy of the model (Khosravi et al, 2018).

In the current study, 13 conditioning factors have been selected, namely slope degree, slope aspect, altitude, plan curvature, stream power index (SPI), topographic wetness index (TWI), Terrain roughness index (TRI), distance from fault, distance from river, land-use/land-cover, rainfall, soil order, and lithology units. These factors have been determined based on literature review, characteristics of the study area, and data availability (Nampak et al., 2014; Mukherjee, 1996; Oh et al., 2011; Ozdemir, 2011b). The process of converting continuous variables into categorical classes were carried out based on our frequency analysis of springs location (Khosravi et al, 2018) in order to define the class intervals.

Digital Elevation Model (DEM) for the study area was downloaded from ASTER global DEM (https://asterweb.jpl.nasa.gov/gdem.asp) with 30x30 m grid size. Based on the DEM, slope degree, slope aspect, altitude, plan curvature, SPI, TWI and TRI were derived. Slope degree has been divided in five categories using the quantile classification scheme (Tehrany et al., 2013, 2014), namely 0-5.5, 5.5-12.11, 12.11-19.4, 19.4-28.7, 28.7-64.3 degrees (Figure 3a). Slope aspect is selected because it controls solar radiation budgets that influence the groundwater potential. Slope aspect has been provided in 5 different classes, flat, north, west, south and east (Figure 3b). Altitude was divided into five classes using the quantile classification scheme, namely 531-1070, 1070-1385, 1385-1703, 1703-2068 and 2068-3175 m (Figure 3c). Plan curvature was divided into three classes, namely concave (<−0.05), flat (−0.05–0.05), and convex (>0.05) (Figure 3d) (Pham et al. 2017).

SPI is related to erosive power of surface runoff, whereas TWI relates to amount of the flow that accumulates at any point in the catchment. In this research, SPI, TWI and TRI were constructed using the System for Automated Geoscientific Analyses SAGA-GIS 2.2 software, and finally, were divided into five classes. These classes are 0-48664, 48664-227099, 227099-583969, 583969-1330153, and 1330153-4136452 for SPI (Figure 3e). For TWI, these classes are 2.1-4.6, 4.6-5.6, 5.6-6.6, 6.6-7.9, 7.9-11.9 (Figure 3f), and for TRI, these classes are 0-8.7, 8.7-18.2, 18.2-29.9, 29.9-46.6, 46.6-185 (Figure 3g).

Distance from fault and river for the study area were generated with five classes using the multiple ring-buffer tool in ArcGIS10.2, 0-200, 200-500, 500-1000, 1000-2000 and >2000 m (Figures 3h and 3i). Lithology plays a key role in determining the groundwater potential due to different infiltration rate of formation (Adiat et al., 2012; Nampak et al., 2014). Land-use/land-cover of the study area was obtained using Landsat 7 Enhanced Thematic Mapper plus (ETM+) images that are downloaded from the US Geological Survey (available at https://earthexplorer.usgs.gov). Accordingly, 25 land-use/land-cover types were recognized: agriculture (A), garden (G), dense-forest (DF), good rangeland (GR), poor forest (PF), waterway (W), mixture of garden and agriculture (MGA), mixture of agriculture with dry farming (MADF), mixture of agriculture with poor-garden (MAPG), dry farming (DF), follow (F), dense rangeland (DR), very poor forest (VPF), mixture of waterway and vegetation (MWV), mixture of moderate forest and agriculture (MMFA), mixture of moderate rangeland and agriculture (MMRA), mixture of poor rangeland and follow (MPRF), mixture of low forest and follow (MLFF), wood-land (WL), moderate forest (MF), moderate rangeland (MR), poor rangeland (PR), bare soil and rock (BSR), urban and residential (UR), mixture of very poor forest (MVPF), and rangeland (R) have been identified (Figure 3j).

Rainfall is the major source of recharge to the groundwater. In this research, mean annual rainfall data of 15 years (2000–2015) at 4 rain-gauge stations of the study area was used. The rainfall map (Figure 3k) with five categories (300-400, 400-500, 500-600, 600-700, and 700-800 mm) was generated using Inverse distance weighted method due to lower RMSE (Khosravi et al, 2016a,b). Soil map at scale of 1:50,000 for the study area was provided by the Iranian Water Resources Department (IWRD). The soil types are soil rock outcrop/entisols, rock outcrop/inceptisols, inceptisols, inceptisols/vertisols, and badlands (Figure 3l).

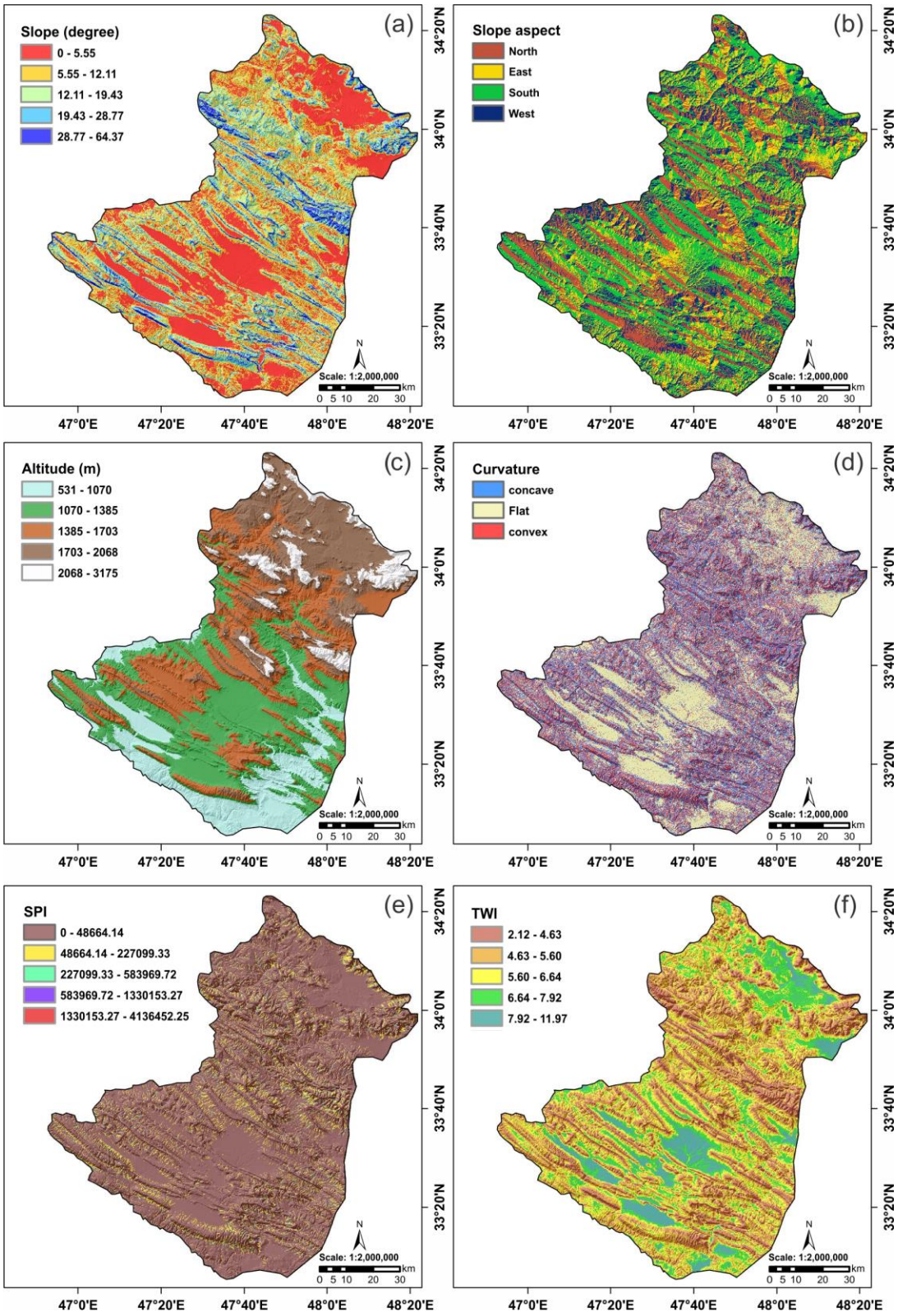

Figure 3. Groundwater conditioning factors for the study area used in this research: (a) slope degree; (b) slope aspect; (c) altitude; (d) plan curvature; (e) SPI; (f) TWI.

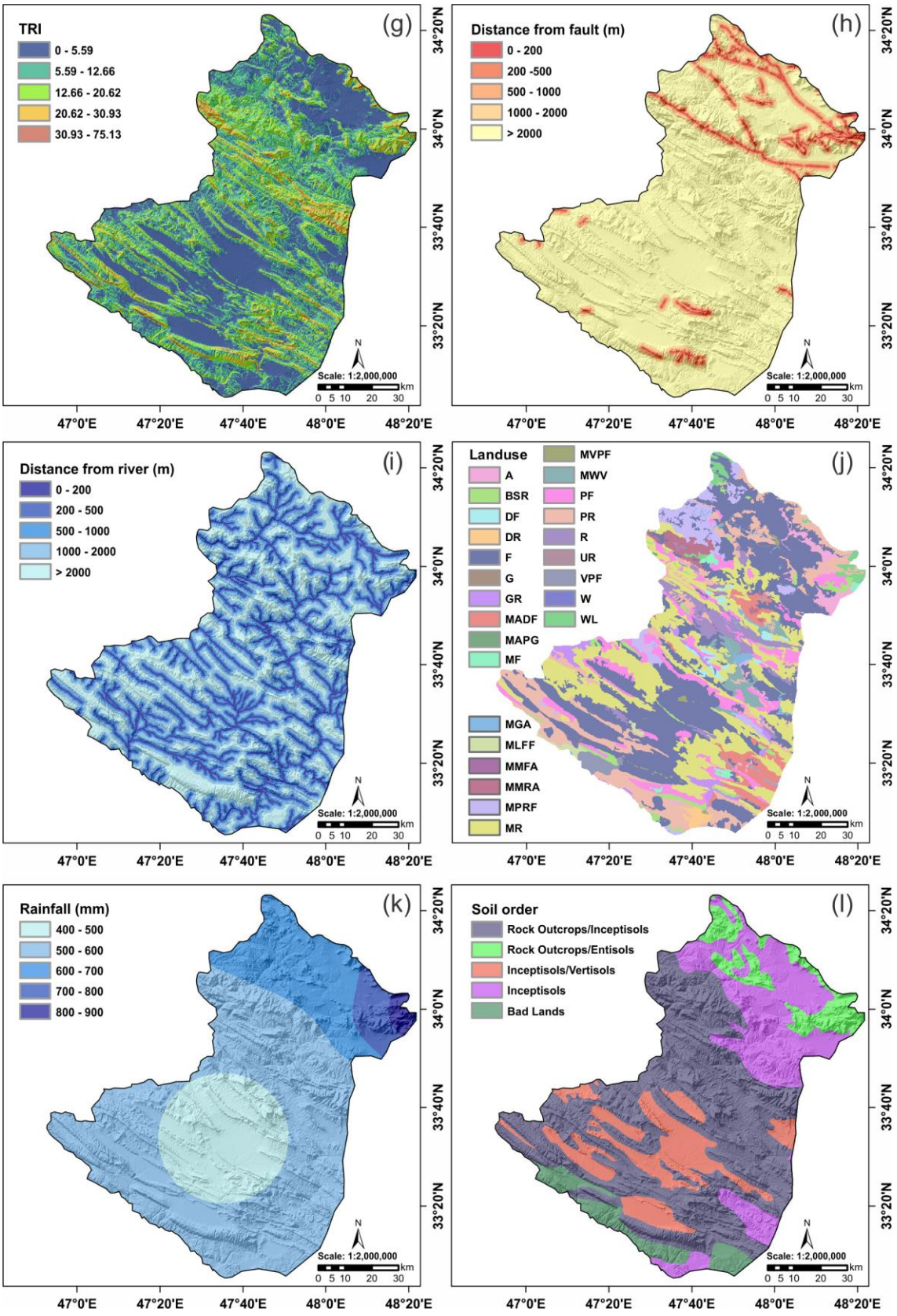
(g)
TRI
0 - 5.59
5.59 - 12.66
12.66 - 20.62
20.62 - 30.93
30.93 - 75.13
(h)
Distance from fault (m)
0 - 200
200 -500
500 - 1000
1000 - 2000
> 2000
(i)
Distance from river (m)
0 - 200
200 - 500
500 - 1000
1000 - 2000
> 2000
(j)
Landuse
A
BSR
DF
DR
F
G
GR
MADF
MAPG
MF
MGA
MLFF
MMFA
MMRA
MPRF
MR
MVPF
MWV
PF
PR
R
UR
VPF
W
WL
(k)
Rainfall (mm)
400 - 500
500 - 600
600 - 700
700 - 800
800 - 900
(l)
Soil order
Rock Outcrops/Inceptisols
Rock Outcrops/Entisols
Inceptisols/Vertisols
Inceptisols
Bad Lands
N
Scale: 1:2,000,000
km
0 5 10 20 30
34°20'N
34°0'N
33°40'N
33°20'N
47°0'E
47°20'E
47°40'E
48°0'E
48°20'E

208

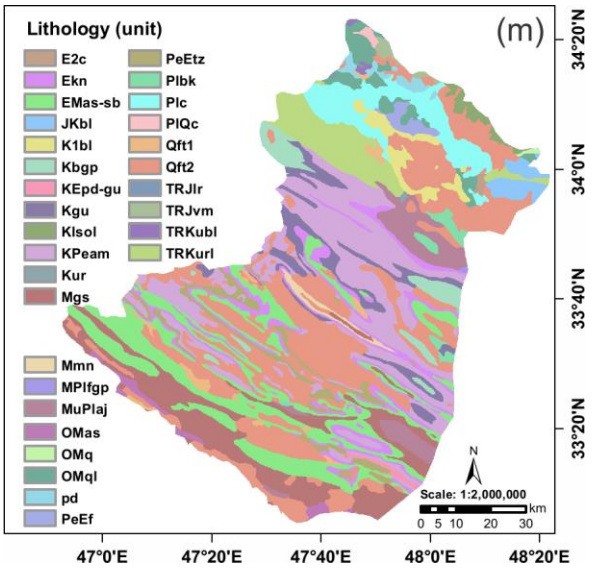

Figure 3. (Continued). (g) TRI; (h) distance from fault; (i) distance from river; (j) land-use/land-cover; (k) rainfall; (l) soil order; and (m) lithology units

Lithology at scale of 1:100000 for the study area was provided by Iranian Department of Geology Survey (IDGS). Accordingly, 30 classes were used: OMq, PeEf, PlQc, K1bl, Plc, pd, TRKubl, TRJvm, MPlfgp, OMql, Plbk, E2c, TRKurl, Qft2, MuPlaj, KEpd-gu, Kgu, Qft1, Ekn, KPeam, PeEtz, Kbgp, EMas-sb, Mgs, TRJlr, Klsol, JKbl, Kur, OMas and Mmn (Figure 3m). Finally, all the aforementioned groundwater conditioning factors for modeling purposes were converted to a raster grid with 30 m × 30 m in the ArcGIS 10.2 software.

3.2. Spatial relationship between spring location and conditioning factors

To assess the spatial relationship between the spring locations and these conditioning factors, in this research, Step-wise Assessment Ratio Analysis (SWARA) (Keršuliene et al., 2010), a Multi-Criteria Decision Making (MCDM) was used. SWARA has received great attention in various fields in the last five years (Alimardani et al., 2013; Hong et al., 2017). The working principal of SWARA was briefly described as follows:

Phase one: first, the experts will define the problem-solving criteria. By using the practical knowledge of the experts, the priority for the criteria is determined and these criteria are organized in descending order.

Phase two: the following trends is employed for estimating the weight for the criteria:

Starting from the second criterion, the respondent explains the relative importance of the criterion j in relation to the $(j-1)$ criterion, and for each particular criterion as well. As Keršuliene mentioned, this process specifies the Comparative Importance of the Average Value, S_j as follows (Keršuliene et al., 2010):

$$S_j = \frac{\sum_1^n A_i}{n} \quad (1)$$

where n is the number of experts; A_i explicates the offered ranks for each factor by the experts; j stands for the number of the factor.

Subsequently, the coefficient K_j is determined as follows:

$$K_j = \begin{cases} 1 & j = 1 \\ S_j + 1 & j > 1 \end{cases} \quad (2)$$

Recalculation of weight Q_j is done as follows:

$$Q_j = \frac{X_{j-1}}{K_j} \quad (3)$$

The relative weights of the evaluation criteria are calculated by the following equation:

$$W_j = \frac{Q_j}{\sum_{j=1}^{m} Q_j} \quad (4)$$

where W_j shows the relative weight of j-th criterion, and m is the total number of criteria.

3.3. Groundwater spring prediction modeling

As mentioned earlier, in this research, five new metaheuristic optimization algorithms (IWO, DE, FA, PSO, and BA) were investigated for optimizing the parameters of ANFIS. This section briefly presents the theoretical background of these algorithms and ANFIS.

3.3.1. Adaptive Neuro-Fuzzy Inference System

Adaptive Neuro-Fuzzy Inference System (ANFIS) was proposed by Jang (1993) to solve nonlinear and complex problems in one framework. ANFIS convert input data to fuzzy inputs by using membership function, Also, there are a different membership functions that describing the system behavior (Jang, 1993). ANFIS applies to the Takgi-Sugeno-Kang (TSK) fuzzy model with two "If-Then" rules both having two inputs x_1 and x_2, and one output f (Takagi and Sugeno, 1985), as follows:

$$Rule\ 1: if\ x_2\ is\ A_2\ and\ x_2\ is\ B_2, then\ f_2 = p_2x_2 + q_2x_2 + r_2 \quad (5)$$

$$Rule\ 2\ 1: if\ x_1\ is\ A_1\ and\ x_2\ is\ B_1, then\ f_1 = p_1x_1 + q_1x_2 + r_1 \quad (6)$$

Jang's ANFIS consists of feed-forward neural network with six distinct layers. Detailed description of ANFIS can be seen in (Jangs, 1993).

3.3.2. Meta-heuristic optimization algorithms

The main goal of these algorithms is to find the optimal antecedent and the consequent parameters of the ANFIS model using IWO, DE, FA, PSO, and BA algorithms. Figure 4 illustrates a general methodological data flow of the ANFIS model.

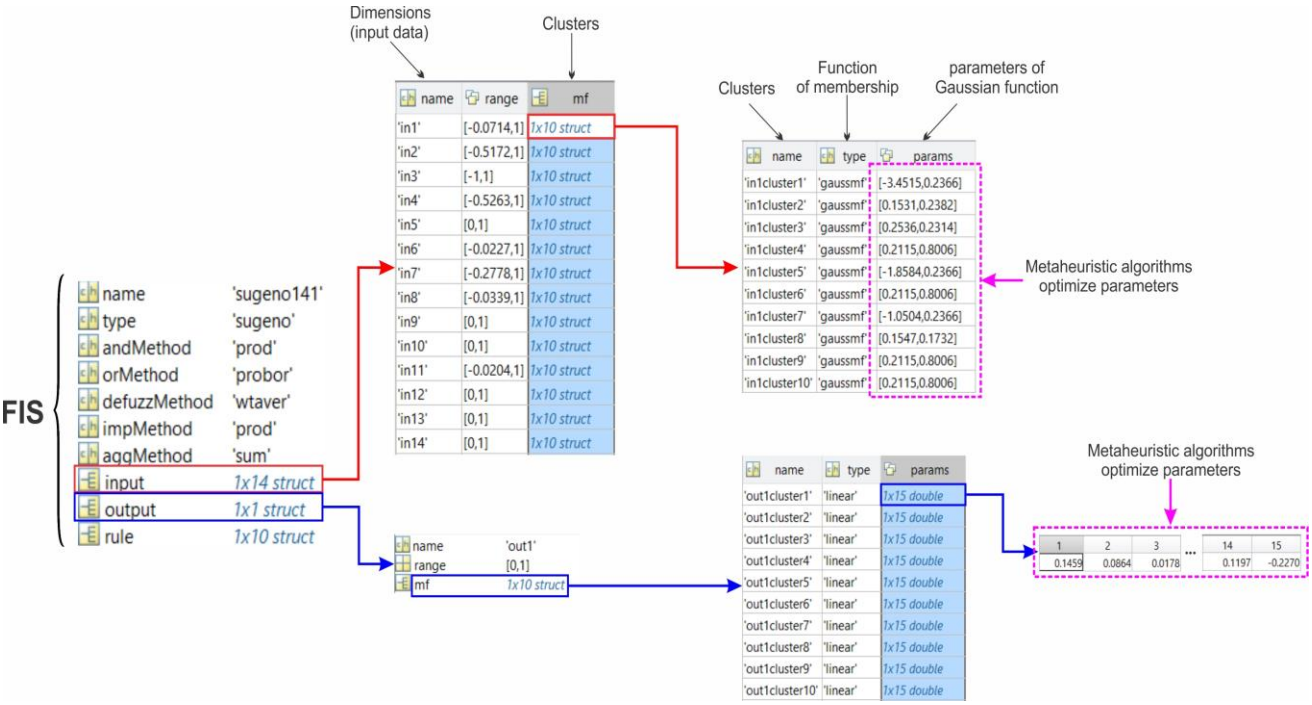

Figure 4. General methodological flow of ANFIS.

3.3.2.1. Invasive Weed Optimization algorithm

Invasive weed optimization (IWO) mimics the colonizing behavior of weeds. Its design is based on the way to find proper place for growth and reproduction of weeds by Mehrabian and Lucas (2006). One characteristic of this algorithm is its simple structure; the number of input parameters is low and it has strong robustness. Furthermore, it is easy to understand and the same merit causes it to be used for solving difficult nonlinear optimization problems (Ghasemi et al., 2014; Naidu and Ojha, 2015; Zhou et al., 2015). This algorithm consists of 4 parts: initialization, reproduction, spatial dispersal, competitive exclusion and termination condition.

3.3.2.2. Differential Evolution algorithm

Differential Evolution (DE) is an evolutionary algorithm for finding global optimal answers for problems with continuous space (Das et al., 2009). This algorithm starts by producing a random population in which each individual of the population is a solution to the problem. Vector $X_i^G = (x_{1,i}^G, x_{2,i}^G, x_{3,i}^G, \dots, x_{D,i}^G)$ shows each individual of the population, $i = \{0,1,2, \dots, NP\}$ is a number denoting each individual, in which D stands for the search dimension, or in other words, is a component problem and $G = \{0,1,2, \dots, G_{max}\}$ generation time that G_{max} is the total number of generations.

By assuming the maximum and minimum of every dimension of searching space, there are $X_L = (x_{1,L}, x_{2,L}, \dots, x_{D,L})$ and $X_U = (, x_{2,U}, \dots, x_{D,U})$, respectively; initial population is defined as the following (Storn and Price, 1997):

$$x_{j,i}^0 = x_{j,L} + rand(0,1).(x_{j,U} - x_{j,L}) \quad (7)$$

where $\mathrm{rand}(0,1)$ is a uniformly distributed random number in [0, 1]. Detailed description of DE can be seen in (Chen et al., 2017a).

3.3.2.3. Firefly Algorithm

Firefly Algorithm (FA) is as a meta-heuristic algorithm that is originated from flashing and communication behavior of fireflies proposed by Yang (2010). Like other swarm intelligence algorithms, where their components are known as solutions for the problems, in this algorithm, each firefly is a solution and its light intensity is the objective function value. In general, FA algorithm follows three idealized rules as below: (1) All firefly species are unisex, with each of them attracting other fireflies without considering their gender (Amiri et al., 2013); (2) Attractiveness of a firefly is related to its light intensity, and thus, from two flashing firefly species, one with lower light intensity moves toward the other one with higher light intensity; (3) Light intensity of a firefly is defined as an objective function value and must be optimized.

3.3.2.4. Particle Swarm Optimization algorithm

Particle Swarm Optimization (PSO) algorithm has been inspired by the way birds use their collective intelligence for finding the best way to get food (Kennedy and Eberhart, 1995). Each bird implemented in this algorithm acts as a particle that is in fact a representative of a solution to the problem. These particles find the optimum answers for the problem by searching in "n" dimensional space, whereas "n" is the number of the problem's parameters. For this purpose, particles were scattered randomly in space at the beginning of algorithm execution. Detailed description of PSO can be seen in Kennedy (2011)

3.3.2.5. Bee algorithm

Bee algorithm (BA), which was introduced by Pham (Pham et al., 2005), is inspired by foraging behavior of bees' colonies in search of food sources located near the hive. In the initial setup, evenly distributed scout bees are scattered randomly in different directions to identify flower patches. After that, scout bees come back to hive and start a specific dance called the waggle dance. This dance is for communicating with others in order to share the information of discovered flower patches. The information indicates direction, distance, and nectar quality of the flower patches, and helps the colony to have proper evaluation of all flower patches. After evaluation, scout bees come back to the location of discovered flower patches with other bees, named recruit bees. Dependent on the distance and the amount of nectar, different number of recruit bees is assigned to each flower patch. In other words, those flower patches with better nectar quality dedicate more recruit bees to themselves. Recruit bees then evaluate the quality of flower patches when performing the harvest process, and leave the flower patches having low quality. Conversely, if the flower patch quality is good, it will be announced during the next waggle dance.

3.4. Performance assessment of models

According to Chung and Fabbari (Chung and Fabbri, 2003), without validation, the result (achieved maps) of the models do not have any scientific significance. Prediction capability of these five spatial groundwater models must be evaluated using both success-rate and prediction-rate curves (Hong et al., 2015). Success-rate curves show how suitable the built model is for the groundwater potential assessment (Gaprindashvili et al., 2014). Success-rate curves have been constructed using groundwater potential maps and the number of spring locations used in training dataset (Pradhan et al. 2010). Prediction rate curves constructed using testing dataset demonstrate how good the model is and evaluate the prediction power of the models.

Therefore, it can be used for model prediction capabilities (Brenning, 2005). The area under the curve (AUC) of success and prediction rate is the base for assessment accuracy of the groundwater potential models quantitatively (Khosravi et al., 2016a; Khosravi et al., 2016b; Pham et al., 2017b). The AUC value varies from 0.5 to 1; the higher the AUC, the better the prediction capability of models.

In addition, Mean Squared Error (MSE) was further used (Tien Bui et al, 2016) as follows:

$$MSE = \frac{\sum_{i=1}^{n}(O_i - E_i)^2}{N} \quad (8)$$

where O_i and E_i are observation (target) and prediction (output) values in both training and testing dataset and N is the total samples in the training or the testing dataset.

3.5. Inferential statistics

3.5.1 Friedman test

Non-parametric statistical procedures such as Freidman test (Friedman, 1937) can be used regardless of statistical assumptions (Derrac et al., 2011) and do not presuppose the data to be normally distributed. The main aim of this test is to find whether there is a significant difference between the performed models or not. In other words, performing multiple comparisons to detect significant differences between the behaviors of two or more models (Beasley and Zumbo, 2003). The null hypothesis (H0) is that there are no differences among the performance of the groundwater potential models. The higher the P-value, the higher the probability that the null hypothesis is not true since if the p-value is less than the significance level (α=0.05), the null hypothesis will be rejected.

3.6.2 Wilcoxon signed-rank test

Because Freidman test only illustrates whether there is any difference between the models or not, this test does not provide pairwise comparisons among compared models. Therefore, another non-parametric statistical test named Wilcoxon signed-rank test have been applied. To evaluate the significance of differences between the performed groundwater potential models, the P value and Z value have been used.

4. Result and analysis

4.1. Multi-collinearity diagnosis

Result of the multi-collinearity analysis in this study is shown in Table 1. The analysis revealed that as VIF is less than 5 and the tolerance is greater than 0.1 indicating no multi-collinearity problem exists among conditioning factors.

Table.1 Multi-collinearity analysis for conditioning factors.

No	Groundwater conditioning factor	Collinearity Statistics	
		Tolerance	VIF
1	Slope degree	0.231	2.401
2	Slope aspect	0.206	4.270
3	Altitude	0.801	2.097
4	Plan curvature	0.513	1.446
5	SPI	0.410	1.689
6	TWI	0.541	2.113
7	TRI	0.328	1.939
8	Distance from fault	0.408	2.25
9	Distance from river	0.212	3.126
11	Land-use/land-cover	0.296	3.891
12	Rainfall	0.298	1.686
13	Soil order	0.205	4.039
10	Geology (Unit)	0.215	4.150

4.2. Determination of the most important parameters

The most common method of Information Gain Ratio (IGR) was applied to identification of the most important conditioning factors. Result shows that all thirteen conditioning factors are effective on groundwater occurrences. The land-use/land-cover factor has the most important impact on groundwater (IGR=0.502) followed by lithology (IGR=0.465), rainfall (IGR=0.421), TWI (IGR=0.400), soil (IGR=0.370), TRI (IGR=0.337), slope degree (IGR=0.317), altitude (IGR=0.287), distance to river (IGR=0.139), aspect (IGR=0.066), plan curvature (IGR=0.0548), distance to fault (IGR=0.0482) and SPI (IGR=0.0323).

4.3. Spatial relationship between springs and the conditioning factors by SWARA method

The spatial correlation between the groundwater springs and the conditioning factors is shown in Table 2 (in the appendix). Regarding the slope, the class of 0-5.5 degree shows the highest probability (0.45) on spring groundwater occurrences. As the slope degree increases, the probability of spring occurrence is reduced. In the case of slope aspect, the east aspect (0.44) has the most impact on spring occurrences. According to calculated results, in terms of altitude, the springs are the most abundant in the altitude of 1703-2068 m (0.6). The SWARA model is high in flat areas (0.4), followed by concave (0.38) and convex (0.2). For SPI, the highest SWARA value is found for the classes of 583969-1330153 (0.46). In the case of the TWI, the SWARA values decrease when the TWI reduces. There is an inverse relationship between TRI and SWARA value, and as the TRI increases, the SWARA value reduces.

Regarding distance from the fault, distance less than 2000 m has the highest impact on spring occurrences and with increase in the distance (greater than 2000 m), the probability of spring occurrence is reduced. Regarding distance to river, it can be seen that the class of 0-200 m has the highest correlation with the spring occurrence (0.46) and there is an inverse relationship between spring occurrence and SWARA values. In the case of land-use, the highest SWARA values are shown for garden areas (0.219), followed by mixture of garden and agriculture (0.17), agricultural areas (0.12), whereas the lowest SWARA is for bare soil and rock (0.00063). The rainfall between 500 and 600 mm has the highest SWARA value (0.61). The inceptisols class has

the highest SWARA values (0.5) followed by rock outcrop/entisols (0.39), rock outcrop/inceptisols (0.056), inceptisoils/Vertisoils (0.028), and badlands (0.014). The highest probability belongs to the highly porous and very good water reservoir karstic oligomiocene and cretaceous pure carbonate formation (OMq and K1bl), the young and poorly consolidated highly porous detrital rock units (PeEf and Plq) and the unconsolidated quaternary alluvium (PlQc).

4.4. Application of ANFIS ensemble models and model's assessment

In the current study, hybrids of ANFIS model and five meta-heuristic algorithms were designed, constructed and implemented in MATLAB 8.0 software. These models were built using the training dataset. Weights gained by the SWARA method for each conditioning factor was fed as the input for training dataset. The result is shown in Figures 5 and 6.

As it can be seen in Figure 5, MSE of the ANFIS-IWO model, the ANFIS-DE model, the ANFIS-FA model, the ANFIS-PSO model, and the ANFIS-BA model using the training dataset are 0.066, 0.066, 0.066, 0.049, and 0.09, respectively. This indicates that the ANFIS-PSO model has the highest performance, whereas the ANFIS-BA model presents the lowest one. The prediction performance of the five models using the validation dataset is shown in Figure 6. MSE of the ANFIS-IWO model, the ANFIS-DE model, the ANFIS-FA model, the ANFIS-PSO model, and the ANFIS-BA model are 0.060, 0.060, 0.060, 0.045, and 0.09, respectively. Therefore, it could be concluded that the ANFIS-PSO model and ANFIS-BA model have the highest and lowest prediction performances, respectively.

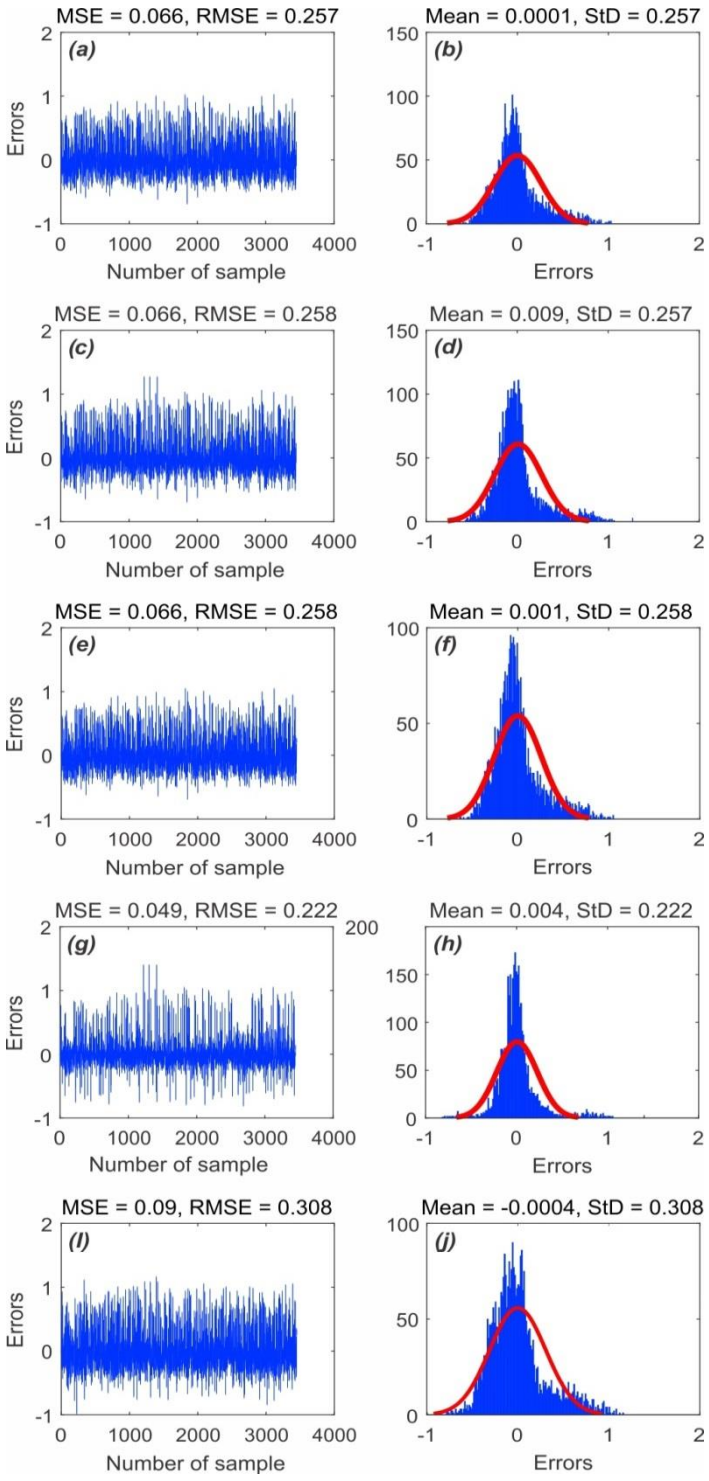

415

416 **Figure 5**. MSE and RMSE values of the five models using the training dataset of: (a) ANFIS-
417 IWO; (c) ANFIS-DE; (e) ANFIS-FA; (g) ANFIS-PSO; and (l) ANFIS-BA. Frequency errors of
418 the five models using the train dataset: (b) ANFIS-IWO; (d) ANFIS-DE; (f) ANFIS-FA; (h)
419 ANFIS-PSO; and (j) ANFIS-BA.

420

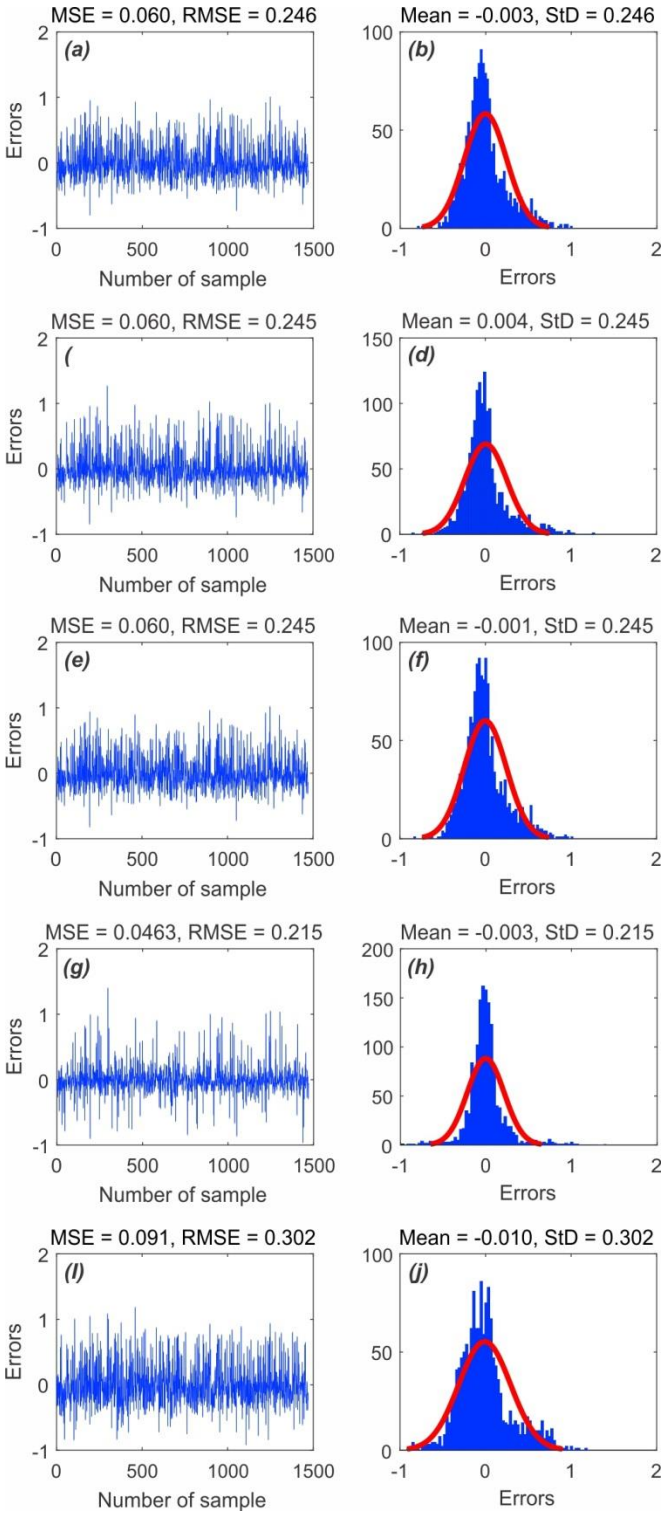

421

422 **Figure 6**. MSE and RMSE values of the five models using the validation dataset: (a) ANFIS-
423 WO; (c) ANFIS-DE; (e) ANFIS-FA; (g) ANFIS-PSO; and (l) ANFIS-BA. Frequency errors of
424 the five models using the validation dataset: (b) ANFIS-IWO; (d) ANFIS-DE; (f) ANFIS-FA;
425 (h) ANFIS-PSO; and (j) ANFIS-BA.

426 However, it should be noticed that, in addition to accuracy, the execution speed of the five
427 models was found significance. To measure this, the running time for 1000 iteration was
428 estimated. The result is shown in Figure 7. It could be seen that the running time of the ANFIS-
429 IWO model, the ANFIS-DE model, the ANFIS-FA model, the ANFIS-PSO model, and the
430 ANFIS-BA model was 8036, 547, 22111, 1050, and 6993 seconds, respectively. It can be
431 concluded that the ANFIS-DE model had the lowest running time and the ANFIS-FA model had
432 the maximum time.

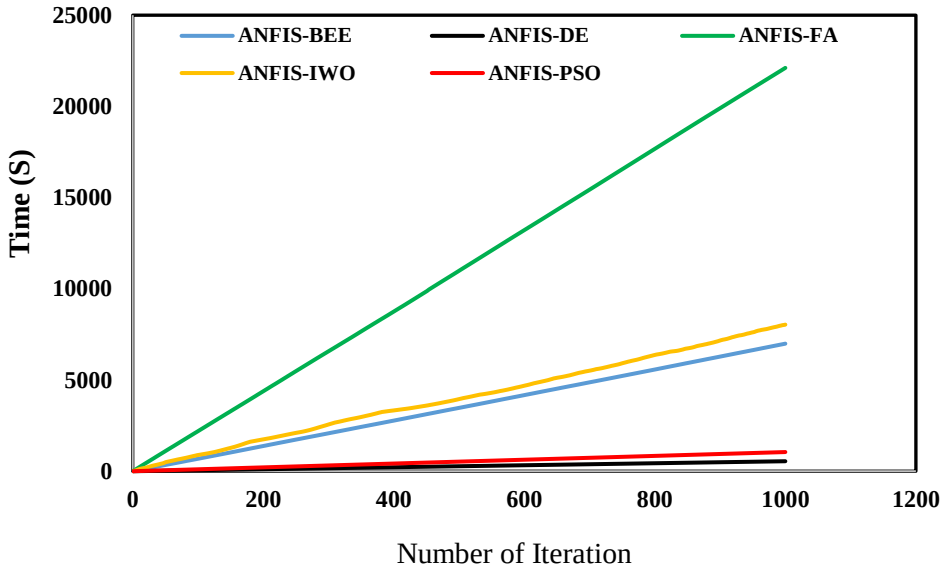

433

434 **Figure 7**. Processing time used for training the five models.

435 On the other hand, it is possible to test how each model achieves convergence in learning. Using
436 the cost function values, a convergence graph for all five models was constructed and shown in
437 Figure 8. The results show that cost function values of the ANFIS-DE model and the ANFIS-BA
438 model were stable from 30 and 95 iterations, indicating a rapid convergence of the models.
439 While the ANFIS-PSO model, the ANFIS-IWO model, and the ANFIS-FA model showed a
440 convergence after 650, 650, and 360 iterations, respectively. This indicates a slow convergence.

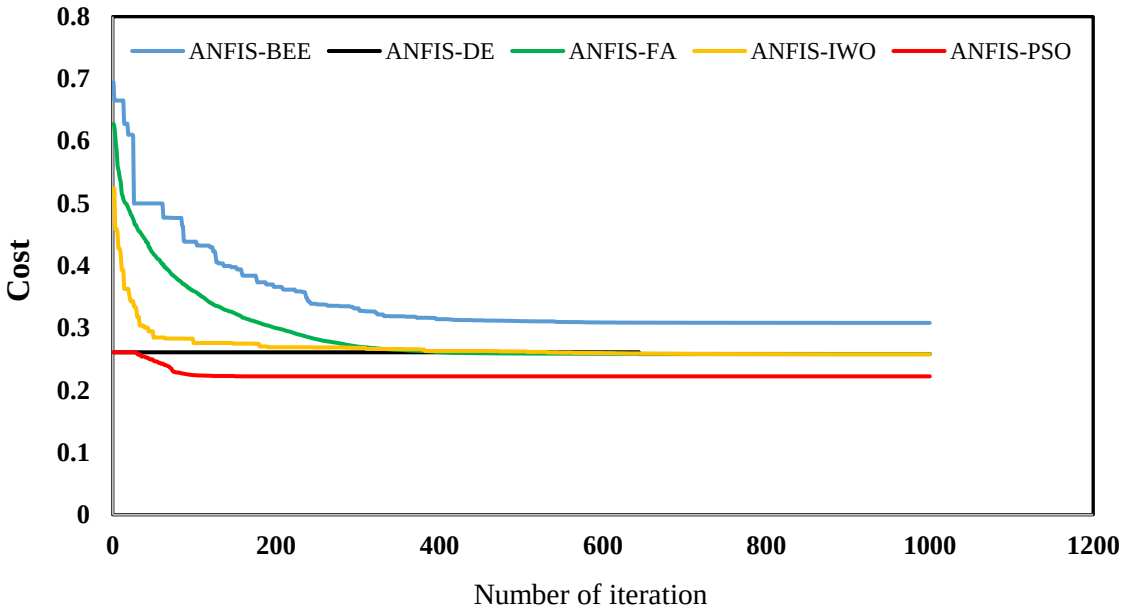

Figure 8. Convergence plot of the models

4.5. Generation of groundwater spring potential maps using ANFIS hybrid models

Once the five models were successfully trained and validated, these models were used to compute groundwater spring indices for all the pixels of the study areas. Then, these indices were exported from MATLAB into ArcGIS10.2 software for generating groundwater spring potential maps. Ultimately, the achieved maps were visualized by five classes: very low, low, moderate, high and very high (Figures 9a, 9b, 9c, 9d, and 9e).

Many methods can be used for determining thresholds for the five classes, manual, equal interval, geometric interval, quantile, natural break and standard deviation. Selection of a method depends on the characteristics of the data and the distribution of the groundwater spring indexes in a histogram (Ayalew and Yamagishi, 2005). If the indexes have a positive or negative skewness, the quantile or natural break classification is proper for indexes classification (Akgun, 2012). In this research, the histogram was checked and the results revealed that the quantile method was better than other methods for index classification.

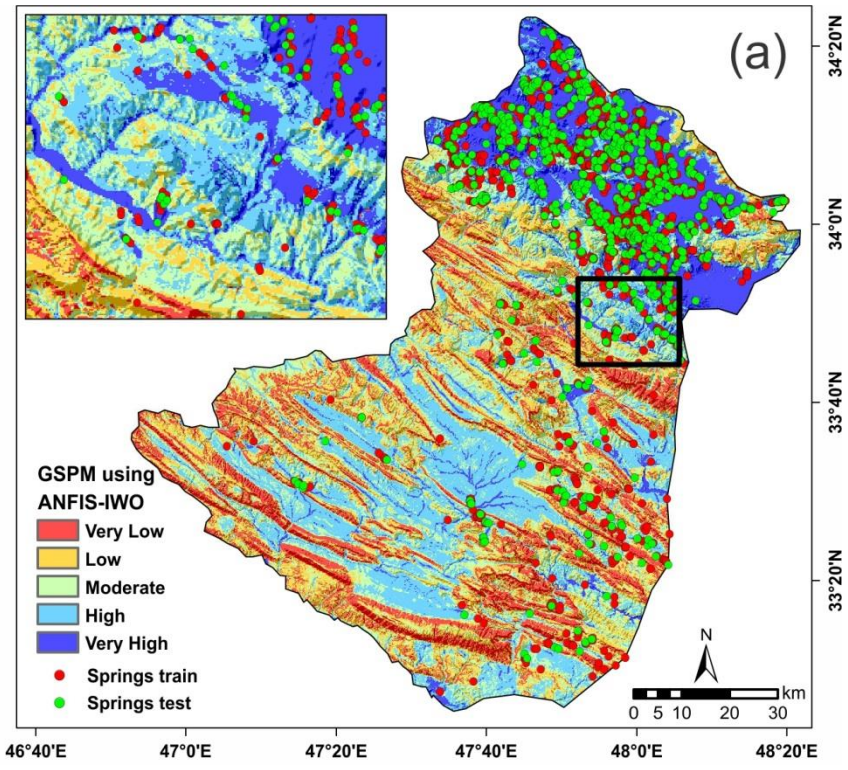
(a)
GSPM using
ANFIS-IWO
Very Low
Low
Moderate
High
Very High
Springs train
Springs test
N
km
0 5 10 20 30
34°20'N
34°0'N
33°40'N
33°20'N
46°40'E
47°0'E
47°20'E
47°40'E
48°0'E
48°20'E

456

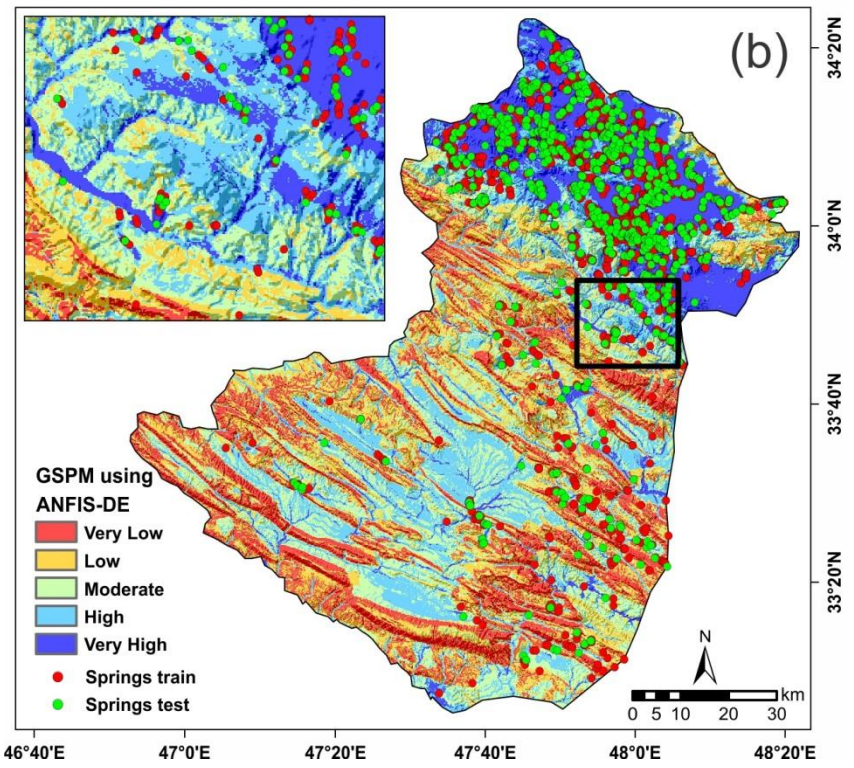
(b)
GSPM using
ANFIS-DE
Very Low
Low
Moderate
High
Very High
Springs train
Springs test
N
km
0 5 10 20 30
34°20'N
34°0'N
33°40'N
33°20'N
46°40'E
47°0'E
47°20'E
47°40'E
48°0'E
48°20'E

457

458

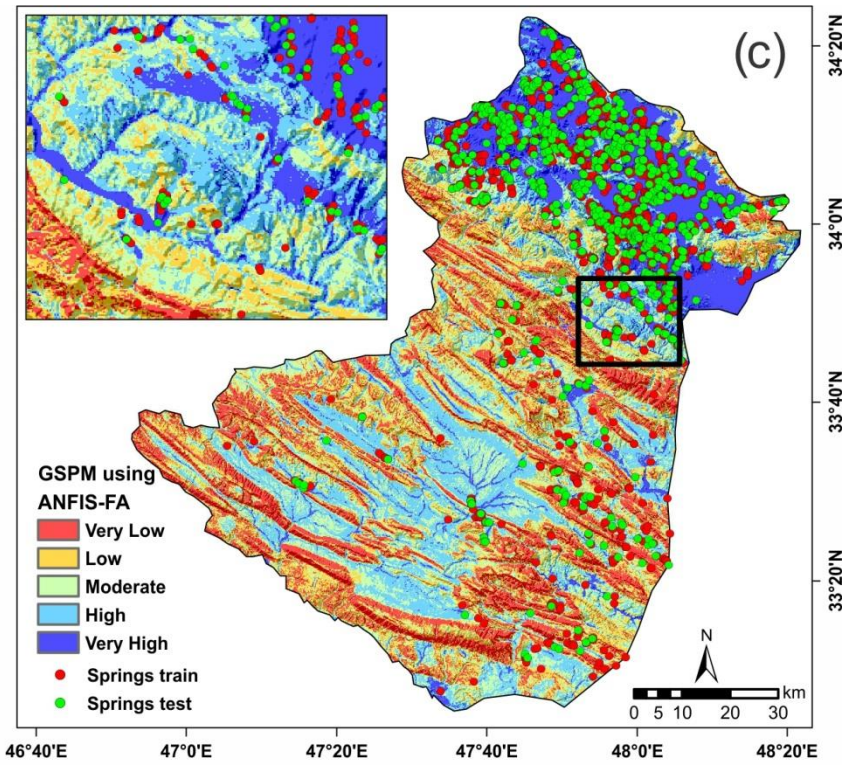
(c)
GSPM using
ANFIS-FA
Very Low
Low
Moderate
High
Very High
Springs train
Springs test
N
km
0 5 10 20 30
34°20'N
34°0'N
33°40'N
33°20'N
46°40'E
47°0'E
47°20'E
47°40'E
48°0'E
48°20'E

459

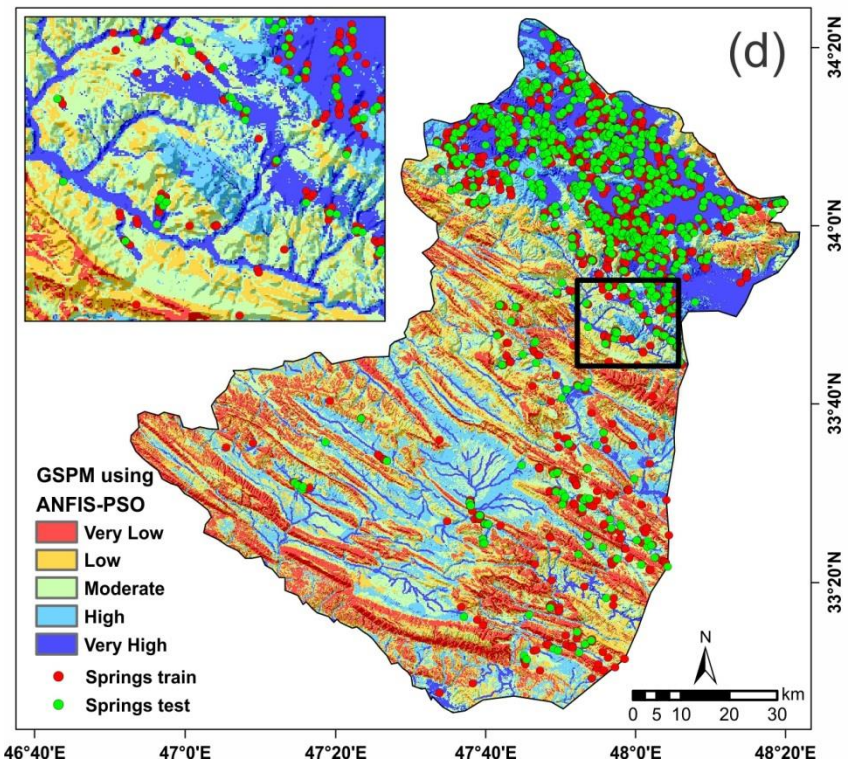
(d)
GSPM using
ANFIS-PSO
Very Low
Low
Moderate
High
Very High
Springs train
Springs test
N
km
0 5 10 20 30
34°20'N
34°0'N
33°40'N
33°20'N
46°40'E
47°0'E
47°20'E
47°40'E
48°0'E
48°20'E

460

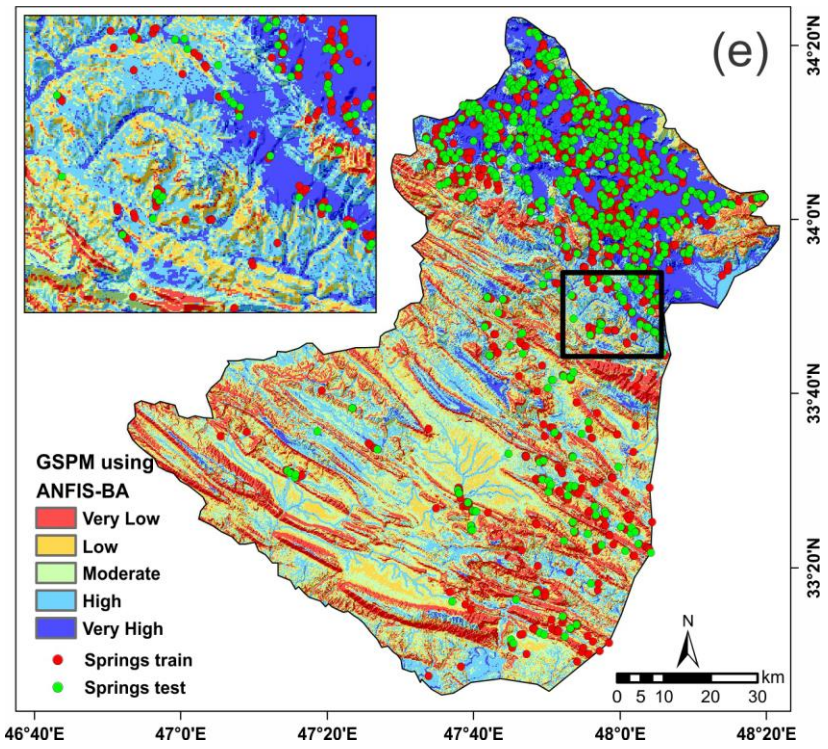

Figure 9. Groundwater spring potential map using: (a) the ANFIS-IWO model; (b) the ANFIS-DE model; (c) the ANFIS-FA model; (d) the ANFIS-PSO model; and (e) the ANFIS-BA model.

4.6. Validation and comparisons of the groundwater spring potential map

The prediction ability and reliability of the five achieved maps have been evaluated using both the training and the validating datasets. The results of the success rate revealed that the ANFIS-DE model had the highest AUC value (0.883) followed by the ANFIS-IWO model (0.882), the ANFIS-FA model (0.882), the ANFIS-PSO model (0.871), and the ANFIS-BA model (0.852) (Figure 10a). Regarding the prediction rate, all five models had a good prediction capability but the ANFIS-DE model has the highest prediction rate (0.873) followed by the NFIS-IWO model (0.873) and the ANFIS-FA model (0.873), the ANFIS-PSO model (0.865), and the ANFIS-BA model (0.839), respectively (Figure 10b).

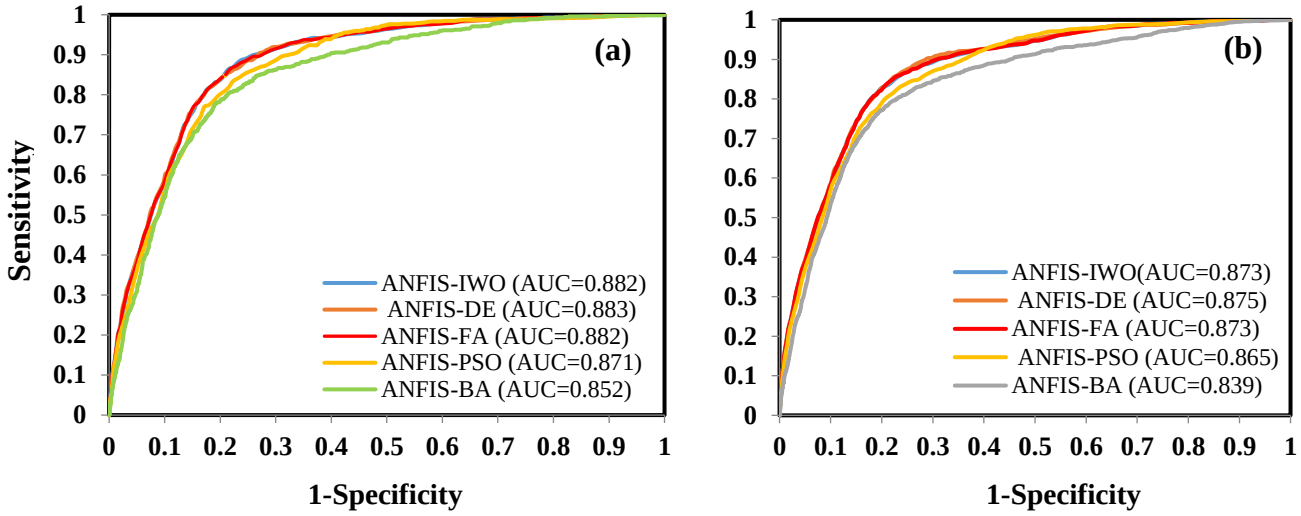

Figure 10. (a) Success rate and (b) prediction rate of the five models.

4.7. Statistical tests

The result of the Friedman test (Table.3) revealed that as Sig and chi-square values were less than 0.05 and greater than 3.84, respectively, the null hypothesis has been rejected. The result also indicated that there was a statistically significant difference between prediction capabilities of the five models.

Table 3. Result of Freidman test.

No	Performed models	Mean rank	Chi-square	Sig
1	ANFIS-DE	3.04	64.84	0.00
2	ANFIS-IWO	3.13		
3	ANFIS-FA	2.98		
4	ANFIS-PSO	2.72		
5	ANFIS-BA	3.12		

The results of the Wilcoxon signed-rank test showed that both P-values and *z*-values were far from the standard values of 0.05 and (from -1.96 to + 1.96), respectively, except for the ANFIS-FA model vs. the ANFIS-DE model and the ANFIS-PSO model vs. the ANFIS-DE model (Table 4). This indicates that there are statistically significant differences between models performance, except for ANFIS-FA vs. ANFIS-DE and ANFIS-PSO vs. ANFIS-DE.

Table 4. Result of Wilcoxon signed rank test.

No	Pairwise comparison	Z-Value	P-Value	Significance
1	ANFIS-DE vs. ANFIS-BA	-3.97	0.00	Yes
2	ANFIS-FA vs. ANFIS-BA	-2.37	0.017	Yes
3	ANFIS-IWO vs. ANFIS-BA	-2.35	0.018	Yes
4	ANFIS-PSO vs. ANFIS-BA	-3.04	0.002	Yes
5	ANFIS-FA vs. ANFIS-DE	-1.32	0.185	No
6	ANFIS-IWO vs. ANFIS-DE	-3.96	0.00	Yes

7	ANFIS-PSO vs. ANFIS-DE	-0.841	0.41	NO
8	ANFIS-IWO vs. ANFIS-FA	-3.19	0.001	Yes
9	ANFIS-PSO vs. ANFIS-FA	-1.90	0.057	Yes
10	ANFIS-PSO vs. ANFIS-IWO	-2.44	0.015	Yes

4.8. Percentage area

The percentage area of each class of final map resulting from the five hybrid models is shown in Figure 11. According to results of the ANFIS-DE as a most accurate models in groundwater spring potential mapping, the percentage areas of very low, low, moderate, high and very high groundwater spring potential are about 19.06, 19.88, 21.72, 20.55 and 18.78 % of the study area, respectively.

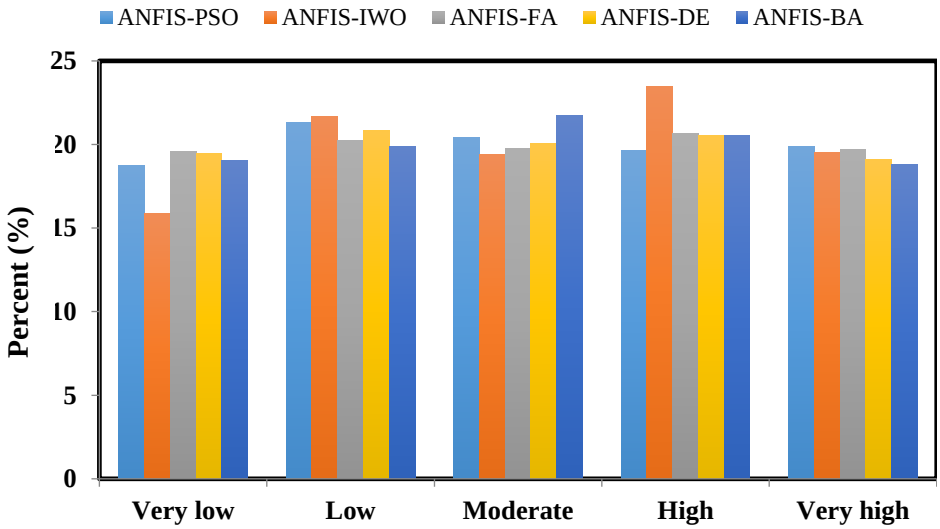

Figure 11. Percentage areas of different groundwater spring potential classes for five models

5. Discussion

5.1. The impact of conditioning factor classes on GSPM

Assessment of conditioning factor is a necessary step in finding the correlation analysis between the groundwater spring and the conditioning factors. It should be noted that no universal guideline is available regarding the number and size of the classes as well as selecting the conditioning factors. They were selected mostly based on characteristics of the study area and previous similar studies (Xu et al., 2013). As the slope increase, the probability of water infiltration reduces and runoff generation will increase. Thus, the steeper the slope, the lower the spring occurrence probability is. According to the result of the SWARA method, the springs almost occur in a middle altitude or mountain slopes. The flat curvature class retains and infiltrates rainfall. Therefore, the amount of groundwater in these areas is higher than concave or convex curvature. The east aspect has more springs than other aspects. These results are in accordance with Pourtaghi and Pourghasemi (2014) who reported that most springs occurred in the elevation of 1600-1900 m and east slope aspect (with FR method).

TWI shows the amount of wetness, and it is obvious that the more the TWI, the higher the groundwater springs probability occurrence is. Terrain Roughness Index (TRI) or topographic

roughness or terrain ruggedness, calculates the sum of change in elevation between a grid cell and its neighborhood, and as the less the roughness, the higher spring potential mapping. The SPI shows the erosive power of the water and mountainous area is higher than plain area. So, as the SPI increases, the spring potential occurrence increases. Rivers are one of the most important sources of groundwater recharge and the nearer to river, the higher probability to springs occurrences. Also, as the rainfall increases, the higher groundwater springs incident, but in the current study, some other conditioning factors affected the spring occurrences.

Most of the springs were located in the garden land-use/land-cover. Therefore, it can be stated that the gardens have been established near the springs. Pliocene-Quaternary formation in a geologic time scale is newer and Quaternary formation has a high potential to groundwater springs incident due to high permeability. The fault is discontinuity in a volume of rock. Thus, the nearer to the fault, the higher the spring occurrence probability will be. Inceptisols soils are relatively new and are characterized by having only the weakest appearance of horizons, the most abundant on the Earth (https://www.britannica.com/science/Inceptisol) and mostly formed from colluvial and alluvial materials. So, due to high permeability and high rainfall infiltration, they have a high potential for springs occurrences. In the case of lithological unit, there are four suitable rock type as water reservoir based on physical phenomena such as porosity and permeability that consist of: 1. unconsolidated sands and gravels; 2. sandstones; 3. lime-stones; and 4. basaltic lava flows. In this study area lithological units include sedimentary rocks mostly carbonate and detrital rocks with cover of alluvium and minor soil.

5.2. Advantages/disadvantages of the models and performance analysis

The highest accuracy based on MSE in both the training and validating datasets is for the ANFIS-PSO model. However, based on the AUC of the success rate and the prediction rate, the ANFIS-DE model has the highest performance. The problem with MSE comes from the fact that it is based on the error assessment. But the models should be acted upon holistically based on abilities. AUC is based on the true positive (TP), true negative (TN), false positive (FP) and false negative (FN), and therefore is more accurate than RMSE for comparison (Termeh et al., 2018).

ANFIS has a potential to capture the benefits of both neural network and fuzzy logic in a single framework and can be considered as a robust model. ANFIS had some advantages including: (1) much better learning ability, (2) need for fewer adjustable parameters than those required in other neural network structure, (3) allowing a better integration with other control design methods by its networks and is (4) more flexible (Vahidnia et al., 2010; Isanta Navarro, 2013).

Despite several advantages of ANFIS, non-adjutancy of membership function is the biggest disadvantage of this model. Finding the optimal parameter for neural fuzzy model in a membership function is difficult; therefore, the best parameter should be finding other optimization models. This problem was addressed in this paper for being solved by five meta-heuristic algorithms, namely IWO, DE, FA, PSO and BA. .

In the current study, the results showed that DE algorithm optimized the parameter for neural fuzzy model better than the four other algorithms. The main DE algorithm's advantage is its simplicity as it consists of only three parameters called N (size of population), F (mutation parameter) and C (crossover parameter) for controlling the search process (Tvrdık, 2006).

Advantages of DE algorithm can be explained as follows: (1) Ability to handle non-differentiable, nonlinear and multimodal cost functions, (2) parallelizability to cope with computation intensive cost functions, (3) good convergence properties, and (4) random sampling and combining vectors in the present population for creating vectors for the next generation.

Finally, it should be noted that each algorithm has some advantages or disadvantages according to the optimization problems which can be summarized as:

Some of the advantages of IWO include the way of reproduction, spatial dispersal, and competitive exclusion (Mehrabian and Lucas, 2006) as well as the fact that seeds and their parents are ranked together and those with better fitness survive and become reproductive (Ahmed et al., 2014). This algorithm can benefit from combined advantages of retaining the dominant poles and the error minimization (Abu-Al-Nadi et al., 2013).

Bees algorithm doesn't employ any probability approach, but utilizes fitness evaluation to drive the search (Yuce et al., 2013). This algorithm uses a set of parameters that makes it powerful, including the number of scout bees in the selected patches, the number of best patches in the selected patches, the number of elite patches in the selected best patches, the number of recruited bees in the elite patches, the number of recruited bees in the non-elite best patches, the size of neighborhood for each patch, the number of iterations and the difference between the value of first and last iterations.

Firefly Algorithm's (FA) advantages are summarized as: (1) handling highly non-linear, multi-modal optimization problems efficiently, (2) not utilizing velocities (3) ability to be integrated with other optimization techniques as a flexible method, and finally (4) not needing a good initial solution to beginning of its iteration process.

Advantages of Particle Swarm Optimization (PSO) algorithm can be summarized as follows: (1) Particles update themselves with the internal velocity; (2) particles have a memory important to the algorithm, (3) the 'best' particle gives out the information to others, (4) it often produces quality solutions more rapidly than alternative methods, (5) it automatically searches for the optimum solution in the solution space (Wan, 2013).

As a result, there isn't any algorithm which works perfectly for all optimization problems, and each algorithm has a different performance accuracy based on different data. New algorithms, therefore, should be applied, tested and finally the most powerful algorithm should be selected; as the conclusion of the research demands.

5.3. Previous works and future work proposal

Some research has been carried out in groundwater well or spring potential mapping using bivariate statistical models (Nampak et al., 2014; Guru et al., 2017; Al-Manmi and Rauf, 2016) using random forest (Rahmati et al., 2016) and using boosted regression tree and classification and regression tree (Naghibi et al., 2016). The ANFIS-metaheuristic hybrid models have not been used in groundwater potential mapping. However, these hybrid models have proven efficient in flood susceptibility mapping (Bui et al., 2016;Termeh et al., 2018) and landslide susceptibility mapping (Chen et al., 2017). Bui et al. (Bui et al., 2016) ensemble the ANFIS using two optimization models, namely Genetic (GA) and PSO for the identification of flood prone areas in Vietnam. Razavi Termeh et al. (Termeh et al., 2018), used ANFIS-Ant Colony

Optimization, ANFIS-GA and ANFIS-PSO in flood susceptibility mapping of Jahrom basin and stated that ANFIS-PSO had higher prediction capabilities than the two other models. Chen et al (2017) applied three hybrid models, namely ANFIS- Genetic Algorithm (GA), ANFIS-Differential Evolution (DE) and ANFIS-Particle Swarm Optimization (PSO) for identifying the areas prone to landslides in Hanyuan County, China. The results showed that ANFIS-DE had a higher performance (AUC=0.84) followed by ANFIS-GA (AUC=0.82) and ANFIS-PSO (AUC=0.78).

In general, the results of the present study, as well as previous research, find that by applying hybrid models, better results could be achieved for spatial prediction modeling including groundwater potential mapping. The ensembles of ANFIS by meta-heuristic algorithms can be applied for any spatial prediction modeling such as groundwater potential mapping, flood susceptibility mapping, landslide susceptibility assessment, gully occurrences susceptibility mapping and other endeavors at a regional scale and in other areas.

For future work, it is recommended that (1) the water quality of the Koohdasht-Nourabad plain be investigated and the water quality of areas with high potential be determined for different aspects such as drinking, agricultural and industrial activities, and (2) the groundwater vulnerability assessment should be applied by some common methods including DRASTIC model for which the zones with high potential to groundwater occurrences should be preserved against pollution.

6. Conclusion

Groundwater is the most important natural resource in the world and about 25 percent of all fresh water is estimated as groundwater. Thus, the groundwater potential mapping has been considered as one of the most effective methods for the management of groundwater resources for better exploitation. The main result of the present study can be summarized as:

1) The results showed that although all models had good results, but, the ANFIS-DE had the highest prediction power (0.875) followed by ANFIS-IWO and ANFIS-FA (0.873), ANFIS-PSO (0.865) and ANFIS-BA (0.839).

2) According to the results of the SWARA method, most springs existed in an altitude of 1703-2068 m, flat curvature, east aspect, TWI of 6.6-7.9, TRI of 0-8.7, SPI of 583969-1330153, Inceptisols soil, slope of 0-5.5 degree, 0-200 m distance from river, 500-1000 m distance from fault, rainfall between 500-600 mm, in a garden, in a Pliocene-Quaternary lithological age and OMq lithology unit at the case study.

3) Based on the information gain ratio, the most important factors on the groundwater occurrence are land-use/land-cover, lithology, rainfall and TWI. The least important factors are plan curvature, distance to fault and SPI.

4) Based on the ANFIS-DE model, totally 39.33% of the case study have a high and very high groundwater potential placed at north of the case study.

The result of the current study is helpful for Iran Water Resources Management Company (IWRMC) for sustainable management of the groundwater resources. Overall, the maps resulting

from these hybrid artificial intelligence algorithms can be applied for better management of the groundwater resources in the study area.

Acknowledgement

We would like to thank Dr. Bjørn Kristofersen at University of South-Eastern Norway for checking English of the manuscript and also two reviewers and Prof. Dimitri Solomatine, editor of the Journal of hydrology and earth system science for their positive and helpful comment.

References

Abu-Al-Nadi, D. I., Alsmadi, O. M., Abo-Hammour, Z. S., Hawa, M. F., and Rahhal, J. S.: Invasive weed optimization for model order reduction of linear MIMO systems, Applied Mathematical Modelling, 37, 4570-4577, 2013.

Adiat, K., Nawawi, M., and Abdullah, K.: Assessing the accuracy of GIS-based elementary multi criteria decision analysis as a spatial prediction tool–A case of predicting potential zones of sustainable groundwater resources, Journal of Hydrology, 440, 75-89, 2012.

Ahmed, A., Al-Amin, R., and Amin, R.: Design of static synchronous series compensator based damping controller employing invasive weed optimization algorithm, SpringerPlus, 3, 394, 2014.

Akgun, A.: A comparison of landslide susceptibility maps produced by logistic regression, multi-criteria decision, and likelihood ratio methods: a case study at İzmir, Turkey, Landslides, 9, 93-106, 10.1007/s10346-011-0283-7, 2012.

Al-Manmi, D. A. M., and Rauf, L. F.: Groundwater potential mapping using remote sensing and GIS-based, in Halabja City, Kurdistan, Iraq, Arabian Journal of Geosciences, 9, 357, 2016.

Alimardani, M., Hashemkhani Zolfani, S., Aghdaie, M. H., and Tamošaitienė, J.: A novel hybrid SWARA and VIKOR methodology for supplier selection in an agile environment, Technological and Economic Development of Economy, 19, 533-548, 2013.

Amiri, B., Hossain, L., Crawford, J. W., and Wigand, R. T.: Community detection in complex networks: Multi–objective enhanced firefly algorithm, Knowledge-Based Systems, 46, 1-11, 2013.

Ayalew, L., and Yamagishi, H.: The application of GIS-based logistic regression for landslide susceptibility mapping in the Kakuda-Yahiko Mountains, Central Japan, Geomorphology, 65, 15-31, 2005.

Beasley, T. M., and Zumbo, B. D.: Comparison of aligned Friedman rank and parametric methods for testing interactions in split-plot designs, Computational statistics & data analysis, 42, 569-593, 2003.

Berhanu, B., Seleshi, Y., and Melesse, A. M.: Surface Water and Groundwater Resources of Ethiopia: Potentials and Challenges of Water Resources Development, in: Nile River Basin, Springer, 97-117, 2014.

Brenning, A.: Spatial prediction models for landslide hazards: review, comparison and evaluation, Natural Hazards and Earth System Science, 5, 853-862, 2005.

Bui, D. T., Lofman, O., Revhaug, I., and Dick, O.: Landslide susceptibility analysis in the Hoa Binh province of Vietnam using statistical index and logistic regression, Natural hazards, 59, 1413, 2011.

Bui, D. T., Pradhan, B., Revhaug, I., Nguyen, D. B., Pham, H. V., and Bui, Q. N.: A novel hybrid evidential belief function-based fuzzy logic model in spatial prediction of rainfall-induced shallow landslides in the Lang Son city area (Vietnam), Geomatics, Natural Hazards and Risk, 6, 243-271, 2015.

Bui, D. T., Pradhan, B., Nampak, H., Bui, Q.-T., Tran, Q.-A., and Nguyen, Q.-P.: Hybrid artificial intelligence approach based on neural fuzzy inference model and metaheuristic optimization for flood susceptibilitgy modeling in a high-frequency tropical cyclone area using GIS, Journal of Hydrology, 540, 317-330, 2016.

Chen, W., Panahi, M., and Pourghasemi, H. R.: Performance evaluation of GIS-based new ensemble data mining techniques of adaptive neuro-fuzzy inference system (ANFIS) with genetic algorithm (GA),

differential evolution (DE), and particle swarm optimization (PSO) for landslide spatial modelling, CATENA, 157, 310-324, 2017.
Chung, C.-J. F., and Fabbri, A. G.: Validation of spatial prediction models for landslide hazard mapping, Natural Hazards, 30, 451-472, 2003.
Das, S., Abraham, A., Chakraborty, U. K., and Konar, A.: Differential evolution using a neighborhood-based mutation operator, IEEE Transactions on Evolutionary Computation, 13, 526-553, 2009.
David Keith Todd, and Mays, L. W.: Groundwater Hydrology, 2rd Edition, Wiley, New York, 1980.
Derrac, J., García, S., Molina, D., and Herrera, F.: A practical tutorial on the use of nonparametric statistical tests as a methodology for comparing evolutionary and swarm intelligence algorithms, Swarm and Evolutionary Computation, 1, 3-18, 2011.
Emamgholizadeh, S., Moslemi, K., and Karami, G.: Prediction the groundwater level of bastam plain (Iran) by artificial neural network (ANN) and adaptive neuro-fuzzy inference system (ANFIS), Water resources management, 28, 5433-5446, 2014.
Ercin, A. E., and Hoekstra, A. Y.: Water footprint scenarios for 2050: A global analysis, Environment International, 64, 71-82, https://doi.org/10.1016/j.envint.2013.11.019, 2014.
Fashae, O. A., Tijani, M. N., Talabi, A. O., and Adedeji, O. I.: Delineation of groundwater potential zones in the crystalline basement terrain of SW-Nigeria: an integrated GIS and remote sensing approach, Applied Water Science, 4, 19-38, 2014.
Fitts, C. R.: Groundwater science, Academic press, 2002.
Friedman, M.: The Use of Ranks to Avoid the Assumption of Normality Implicit in the Analysis of Variance, Journal of the American Statistical Association, 32, 675-701, 10.1080/01621459.1937.10503522, 1937.
Gaprindashvili, G., Guo, J., Daorueang, P., Xin, T., and Rahimy, P.: A new statistic approach towards landslide hazard risk assessment, International Journal of Geosciences, 5, 38, 2014.
Ghasemi, M., Ghavidel, S., Akbari, E., and Vahed, A. A.: Solving non-linear, non-smooth and non-convex optimal power flow problems using chaotic invasive weed optimization algorithms based on chaos, Energy, 73, 340-353, 2014.
Guru, B., Seshan, K., and Bera, S.: Frequency ratio model for groundwater potential mapping and its sustainable management in cold desert, India, Journal of King Saud University-Science, 29, 333-347, 2017.
Hong, H., Pradhan, B., Xu, C., and Bui, D. T.: Spatial prediction of landslide hazard at the Yihuang area (China) using two-class kernel logistic regression, alternating decision tree and support vector machines, Catena, 133, 266-281, 2015.
Hong, H., Panahi, M., Shirzadi, A., Ma, T., Liu, J., Zhu, A.-X., Chen, W., Kougias, I., and Kazakis, N.: Flood susceptibility assessment in Hengfeng area coupling adaptive neuro-fuzzy inference system with genetic algorithm and differential evolution, Science of The Total Environment, 2017.
Israil, M., Al-Hadithi, M., and Singhal, D.: Application of a resistivity survey and geographical information system (GIS) analysis for hydrogeological zoning of a piedmont area, Himalayan foothill region, India, Hydrogeology journal, 14, 753-759, 2006.
Jang, J.-S.: ANFIS: adaptive-network-based fuzzy inference system, IEEE transactions on systems, man, and cybernetics, 23, 665-685, 1993.
Jha, M. K., Chowdary, V., and Chowdhury, A.: Groundwater assessment in Salboni Block, West Bengal (India) using remote sensing, geographical information system and multi-criteria decision analysis techniques, Hydrogeology journal, 18, 1713-1728, 2010.
Kaliraj, S., Chandrasekar, N., and Magesh, N.: Identification of potential groundwater recharge zones in Vaigai upper basin, Tamil Nadu, using GIS-based analytical hierarchical process (AHP) technique, Arabian Journal of Geosciences, 7, 1385-1401, 2014.
Kennedy, J., and Eberhart, R.: Particle swarm optimization, IEEE International of first Conference on Neural Networks, in, Perth, Australia, IEEE Press, 1995.
Kennedy, J.: Particle swarm optimization, in: Encyclopedia of machine learning, Springer, 760-766, 2011.

731 Keršuliene, V., Zavadskas, E. K., and Turskis, Z.: Selection of rational dispute resolution method by
732 applying new step-wise weight assessment ratio analysis (SWARA), Journal of business economics and
733 management, 11, 243-258, 2010.
734 Khosravi, K., Nohani, E., Maroufinia, E., and Pourghasemi, H. R.: A GIS-based flood susceptibility
735 assessment and its mapping in Iran: a comparison between frequency ratio and weights-of-evidence
736 bivariate statistical models with multi-criteria decision-making technique, Natural Hazards, 83, 947-987,
737 2016a.
738 Khosravi, K., Pourghasemi, H. R., Chapi, K., and Bahri, M.: Flash flood susceptibility analysis and its
739 mapping using different bivariate models in Iran: a comparison between Shannon's entropy, statistical
740 index, and weighting factor models, Environmental monitoring and assessment, 188, 656, 2016b.
741 Khosravi, K., Pham, B.T., Chapi. K., Shirzadi, A., et al., 2018. A comparative assessment of decision
742 trees algorithms for flash flood susceptibility modeling at Haraz watershed, northern Iran. Science of the
743 total environemnt, 627, 744-755, doi.org/10.1016/j.scitotenv.2018.01.266.
744 Li, Y.-F., Xie, M., and Goh, T.-N.: Adaptive ridge regression system for software cost estimating on
745 multi-collinear datasets, Journal of Systems and Software, 83, 2332-2343, 2010.
746 Lohani, A., Kumar, R., and Singh, R.: Hydrological time series modeling: A comparison between
747 adaptive neuro-fuzzy, neural network and autoregressive techniques, Journal of Hydrology, 442, 23-35,
748 2012.
749 Maiti, S., and Tiwari, R.: A comparative study of artificial neural networks, Bayesian neural networks and
750 adaptive neuro-fuzzy inference system in groundwater level prediction, Environmental earth sciences, 71,
751 3147-3160, 2014.
752 Mehrabian, A. R., and Lucas, C.: A novel numerical optimization algorithm inspired from weed
753 colonization, Ecological informatics, 1, 355-366, 2006.
754 Mohanty, S., Jha, M. K., Raul, S., Panda, R., and Sudheer, K.: Using artificial neural network approach
755 for simultaneous forecasting of weekly groundwater levels at multiple sites, Water Resources
756 Management, 29, 5521-5532, 2015.
757 Mukherjee, S.: Targeting saline aquifer by remote sensing and geophysical methods in a part of
758 Hamirpur-Kanpur, India, Hydrogeol J, 19, 53-64, 1996.
759 Naghibi, S. A., Pourghasemi, H. R., Pourtaghi, Z. S., and Rezaei, A.: Groundwater qanat potential
760 mapping using frequency ratio and Shannon's entropy models in the Moghan watershed, Iran, Earth
761 Science Informatics, 8, 171-186, 2015.
762 Naghibi, S. A., Pourghasemi, H. R., and Dixon, B.: GIS-based groundwater potential mapping using
763 boosted regression tree, classification and regression tree, and random forest machine learning models in
764 Iran, Environmental monitoring and assessment, 188, 44, 2016.
765 Naidu, Y. R., and Ojha, A.: A hybrid version of invasive weed optimization with quadratic
766 approximation, Soft Computing, 19, 3581-3598, 2015.
767 Nampak, H., Pradhan, B., and Manap, M. A.: Application of GIS based data driven evidential belief
768 function model to predict groundwater potential zonation, Journal of Hydrology, 513, 283-300, 2014.
769 Nosrati, K., and Van Den Eeckhaut, M.: Assessment of groundwater quality using multivariate statistical
770 techniques in Hashtgerd Plain, Iran, Environmental Earth Sciences, 65, 331-344, 2012.
771 Nourani, V., Alami, M. T., and Vousoughi, F. D.: Hybrid of SOM-Clustering Method and Wavelet-
772 ANFIS Approach to Model and Infill Missing Groundwater Level Data, J. Hydrol. Eng., 21, 05016018,
773 2016.
774 O'brien, R. M.: A caution regarding rules of thumb for variance inflation factors, Quality & Quantity, 41,
775 673-690, 2007.
776 Oh, H.-J., Kim, Y.-S., Choi, J.-K., Park, E., and Lee, S.: GIS mapping of regional probabilistic
777 groundwater potential in the area of Pohang City, Korea, Journal of Hydrology, 399, 158-172, 2011.
778 Ozdemir, A.: Using a binary logistic regression method and GIS for evaluating and mapping the
779 groundwater spring potential in the Sultan Mountains (Aksehir, Turkey), Journal of Hydrology, 405, 123-
780 136, 2011a.

781 Ozdemir, A.: GIS-based groundwater spring potential mapping in the Sultan Mountains (Konya, Turkey)
782 using frequency ratio, weights of evidence and logistic regression methods and their comparison, Journal
783 of Hydrology, 411, 290-308, 2011b.
784 Pham, B. T., Bui, D. T., Pourghasemi, H. R., Indra, P., and Dholakia, M.: Landslide susceptibility
785 assesssment in the Uttarakhand area (India) using GIS: a comparison study of prediction capability of
786 naïve bayes, multilayer perceptron neural networks, and functional trees methods, Theoretical and
787 Applied Climatology, 128, 255-273, 2017a.
788 Pham, B. T., Khosravi, K., and Prakash, I.: Application and comparison of decision tree-based machine
789 learning methods in landside susceptibility assessment at Pauri Garhwal Area, Uttarakhand, India,
790 Environmental Processes, 4, 711-730, 2017b.
791 Pham, D., Ghanbarzadeh, A., Koc, E., Otri, S., Rahim, S., and Zaidi, M.: The bees algorithm. Technical
792 note, Manufacturing Engineering Centre, Cardiff University, UK, 1-57, 2005.
793 Pourghasemi, H., Moradi, H., and Aghda, S. F.: Landslide susceptibility mapping by binary logistic
794 regression, analytical hierarchy process, and statistical index models and assessment of their
795 performances, Natural hazards, 69, 749-779, 2013a.
796 Pourghasemi, H. R., Pradhan, B., and Gokceoglu, C.: Application of fuzzy logic and analytical hierarchy
797 process (AHP) to landslide susceptibility mapping at Haraz watershed, Iran, Natural hazards, 63, 965-996,
798 2012.
799 Pourghasemi, H. R., Pradhan, B., Gokceoglu, C., Mohammadi, M., and Moradi, H. R.: Application of
800 weights-of-evidence and certainty factor models and their comparison in landslide susceptibility mapping
801 at Haraz watershed, Iran, Arabian Journal of Geosciences, 6, 2351-2365, 2013b.
802 Pourghasemi, H. R., and Beheshtirad, M.: Assessment of a data-driven evidential belief function model
803 and GIS for groundwater potential mapping in the Koohrang Watershed, Iran, Geocarto International, 30,
804 662-685, 2015.
805 Pourtaghi, Z. S., and Pourghasemi, H. R.: GIS-based groundwater spring potential assessment and
806 mapping in the Birjand Township, southern Khorasan Province, Iran, Hydrogeology Journal, 22, 643-662,
807 2014.
808 Rahmati, O., Samani, A. N., Mahdavi, M., Pourghasemi, H. R., and Zeinivand, H.: Groundwater potential
809 mapping at Kurdistan region of Iran using analytic hierarchy process and GIS, Arabian Journal of
810 Geosciences, 8, 7059-7071, 2015.
811 Rahmati, O., Pourghasemi, H. R., and Melesse, A. M.: Application of GIS-based data driven random
812 forest and maximum entropy models for groundwater potential mapping: a case study at Mehran Region,
813 Iran, Catena, 137, 360-372, 2016.
814 Richey, A. S., Thomas, B. F., Lo, M. H., Reager, J. T., Famiglietti, J. S., Voss, K., Swenson, S., and
815 Rodell, M.: Quantifying renewable groundwater stress with GRACE, Water resources research, 51, 5217-
816 5238, 2015.
817 Sander, P., Chesley, M. M., and Minor, T. B.: Groundwater assessment using remote sensing and GIS in a
818 rural groundwater project in Ghana: lessons learned, Hydrogeology Journal, 4, 40-49, 1996.
819 Siebert, S., Henrich, V., Frenken, K., and Burke, J.: Update of the digital global map of irrigation areas to
820 version 5, Rheinische Friedrich-Wilhelms-Universität, Bonn, Germany and Food and Agriculture
821 Organization of the United Nations, Rome, Italy, 2013.
822 Singh, A. K., and Prakash, S. R.: An integrated approach of remote sensing, geophysics and GIS to
823 evaluation of groundwater potentiality of Ojhala sub-watershed, Mirjapur district, UP, India, Asian
824 conference on GIS, GPS, aerial photography and remote sensing, Bangkok-Thailand, 2002,
825 Storn, R., and Price, K.: Differential evolution–a simple and efficient heuristic for global optimization
826 over continuous spaces, Journal of global optimization, 11, 341-359, 1997.
827 Sun, Y., Wendi, D., Kim, D. E., and Liong, S.-Y.: Application of artificial neural networks in
828 groundwater table forecasting–a case study in a Singapore swamp forest, Hydrology and Earth System
829 Sciences, 20, 1405-1412, 2016.
830 Takagi, T., and Sugeno, M.: Fuzzy identification of systems and its applications to modeling and control,
831 IEEE transactions on systems, man, and cybernetics, 116-132, 1985.

Tehrany, M. S., Pradhan, B., and Jebur, M. N.: Spatial prediction of flood susceptible areas using rule based decision tree (DT) and a novel ensemble bivariate and multivariate statistical models in GIS, Journal of Hydrology, 504, 69-79, 2013.
Tehrany, M. S., Pradhan, B., and Jebur, M. N.: Flood susceptibility mapping using a novel ensemble weights-of-evidence and support vector machine models in GIS, Journal of hydrology, 512, 332-343, 2014.
Termeh, S. V. R., Kornejady, A., Pourghasemi, H. R., and Keesstra, S.: Flood susceptibility mapping using novel ensembles of adaptive neuro fuzzy inference system and metaheuristic algorithms, Science of the Total Environment, 615, 438-451, 2018.
Tvrdık, J.: Competitive differential evolution and genetic algorithm in GA-DS toolbox, Technical Computing Prague, Praha, Humusoft, 99-106, 2006.
Umar, Z., Pradhan, B., Ahmad, A., Jebur, M. N., and Tehrany, M. S.: Earthquake induced landslide susceptibility mapping using an integrated ensemble frequency ratio and logistic regression models in West Sumatera Province, Indonesia, Catena, 118, 124-135, 2014.
Waikar, M., and Nilawar, A. P.: Identification of groundwater potential zone using remote sensing and GIS technique, Int J Innov Res Sci Eng Technol, 3, 1264-1274, 2014.
Wan, S.: Entropy-based particle swarm optimization with clustering analysis on landslide susceptibility mapping, Environmental earth sciences, 68, 1349-1366, 2013.
Xu, C., Dai, F., Xu, X., and Lee, Y. H.: GIS-based support vector machine modeling of earthquake-triggered landslide susceptibility in the Jianjiang River watershed, China, Geomorphology, 145, 70-80, 2012.
Xu, C., Xu, X., Dai, F., Wu, Z., He, H., Shi, F., Wu, X., and Xu, S.: Application of an incomplete landslide inventory, logistic regression model and its validation for landslide susceptibility mapping related to the May 12, 2008 Wenchuan earthquake of China, Natural hazards, 68, 883-900, 2013.
Yang, X.-S.: Nature-inspired metaheuristic algorithms, Luniver press, 2010.
Yuce, B., Packianather, M. S., Mastrocinque, E., Pham, D. T., and Lambiase, A.: Honey bees inspired optimization method: the bees algorithm, Insects, 4, 646-662, 2013.
Zare, M., and Koch, M.: Groundwater level fluctuations simulation and prediction by ANFIS-and hybrid Wavelet-ANFIS/Fuzzy C-Means (FCM) clustering models: Application to the Miandarband plain, Journal of Hydro-environment Research, 18, 63-76, 2018.
Zhou, Y., Luo, Q., Chen, H., He, A., and Wu, J.: A discrete invasive weed optimization algorithm for solving traveling salesman problem, Neurocomputing, 151, 1227-1236, 2015.

Appendix

Table.2. Spatial correlation between conditioning factors and the spring locations by SWARA methods

Factors	Classes	Comparative importance of average value Kj	Coefficient Kj=Sj +1	wj=(X(j-1))/kj	weight wj/ sigma wj
Slope (degree)	0 - 5.55		1.000	1.000	0.454
	5.55 - 12.11	0.300	1.300	0.769	0.349
	12.11 - 19.43	1.500	2.500	0.308	0.140
	19.43 - 28.77	2.000	3.000	0.103	0.047
	28.77 - 64.37	3.500	4.500	0.023	0.010

	East		1.000	1.000	0.448
	North	1.000	2.000	0.500	0.224
Slope aspect	West	0.300	1.300	0.385	0.172
	South	0.100	1.100	0.350	0.156
	Flat	0.8	1.05	0.31	0.121
	1703 - 2068		1.000	1.000	0.608
	1385 - 1703	2.200	3.200	0.313	0.190
Altitude (m)	2068 - 3175	0.800	1.800	0.174	0.106
	531 - 1070	1.000	2.000	0.087	0.053
	1070 - 1385	0.200	1.200	0.072	0.044
	Flat		1.000	1.000	0.408
Plan curvature	concave	0.050	1.050	0.952	0.388
	convex	0.900	1.900	0.501	0.204
	583969.72 - 1330153.27		1.000	1.000	0.466
	227099.33 - 583969.72	1.000	2.000	0.500	0.233
SPI	48664.14 - 227099.33	0.200	1.200	0.417	0.194
	0 - 48664.14	1.000	2.000	0.208	0.097
	1330153.27 - 4136452.25	10.000	11.000	0.019	0.009
	6.64 - 7.92		1.000	1.000	0.471
	5.60 - 6.64	0.700	1.700	0.588	0.277
TWI	7.92 - 11.97	1.300	2.300	0.256	0.120
	4.63 - 5.60	0.100	1.100	0.233	0.110
	2.12 - 4.63	4.000	5.000	0.047	0.022
	0 - 5.59		1.000	1.000	0.544
	5.59 - 12.66	0.800	1.800	0.556	0.302
TRI	12.66 - 20.62	1.500	2.500	0.222	0.121
	20.62 - 30.93	3.000	4.000	0.056	0.030
	30.93 - 75.13	10.000	11.000	0.005	0.003
	0 - 200		1.000	1.000	0.242
Distance from fault (m)	200 - 500	0.050	1.050	0.952	0.231
	500 - 1000	0.100	1.100	0.866	0.210

	1000 - 2000	0.050	1.050	0.825	0.200
	> 2000	0.700	1.700	0.485	0.118
Distance from river (m)	0 - 200		1.000	1.000	0.464
	200 - 500	1.900	2.900	0.345	0.160
	500 - 1000	0.050	1.050	0.328	0.152
	1000 - 2000	0.300	1.300	0.253	0.117
	> 2000	0.100	1.100	0.230	0.107
Land-use/land-cover	Garden		1.000	1.000	0.219
	Mixture of garden and agriculture	0.282	1.282	0.780	0.171
	Agriculture	0.340	1.340	0.582	0.128
	Mixture of poor rangeland and follow	0.419	1.419	0.410	0.090
	Follow	0.233	1.233	0.333	0.073
	Mixture of moderate rangeland and agriculture	0.294	1.294	0.257	0.056
	Mixture of very poor forest	0.124	1.124	0.229	0.050
	Mixture of waterway and vegetation	0.549	1.549	0.148	0.032
	Moderate forest	0.205	1.205	0.122	0.027
	Mixture of agriculture with dry farming	0.064	1.064	0.115	0.025
	Wood-land	0.030	1.030	0.112	0.024
	Good rangeland	0.043	1.043	0.107	0.023
	Rangeland	0.333	1.333	0.080	0.018
	Poor rangeland	0.030	1.030	0.078	0.017
	Poor forest	0.210	1.210	0.065	0.014
	Moderate rangeland	0.281	1.281	0.050	0.011
	Bare soil and rock	0.237	1.237	0.041	0.009
	Dense rangeland	0.278	1.278	0.032	0.007
	Dense-forest	10.000	11.000	0.003	0.001
	Waterway	0.000	1.000	0.003	0.001
	Mixture of agriculture with poor-garden	0.000	1.000	0.003	0.001

	Very poor forest	0.000	1.000	0.003	0.001
	Mixture of moderate forest and agriculture	0.000	1.000	0.003	0.001
	Mixture of low forest and follow,	0.000	1.000	0.003	0.001
	Urban and residential	0.000	1.000	0.003	0.001
Rainfall (mm)	600 - 700		1.000	1.000	0.617
	700 - 800	2.200	3.200	0.313	0.193
	800 - 900	0.600	1.600	0.195	0.121
	500 - 600	1.500	2.500	0.078	0.048
	400 - 500	1.300	2.300	0.034	0.021
Soil order	Rock Outcrops/Entisols		1.000	1.000	0.509
	Rock Outcrops/Inceptisols	0.300	1.300	0.769	0.392
	Inceptisols	5.900	6.900	0.111	0.057
	Inceptisols/Vertisols	1.000	2.000	0.056	0.028
	Bad Lands	1.000	2.000	0.028	0.014
Lithology (unit)	OMq		1.000	1.000	0.133
	PeEf	0.309	1.309	0.764	0.101
	PlQc	0.253	1.253	0.610	0.081
	K1bl	0.113	1.113	0.548	0.073
	Plc	0.014	1.014	0.541	0.072
	pd	0.059	1.059	0.511	0.068
	TRKubl	0.223	1.223	0.417	0.055
	TRJvm	0.027	1.027	0.406	0.054
	MPlfgp	0.048	1.048	0.388	0.051
	OMql	0.015	1.015	0.382	0.051
	Plbk	0.081	1.081	0.353	0.047
	E2c	0.291	1.291	0.274	0.036
	TRKurl	0.059	1.059	0.258	0.034
	Qft2	0.335	1.335	0.194	0.026
	MuPlaj	0.100	1.100	0.176	0.023
	KEpd-gu	0.080	1.080	0.163	0.022

Kgu	0.566	1.566	0.104	0.014
Qft1	0.064	1.064	0.098	0.013
Ekn	0.109	1.109	0.088	0.012
KPeam	0.027	1.027	0.086	0.011
PeEtz	0.328	1.328	0.065	0.009
Kbgp	0.445	1.445	0.045	0.006
EMas-sb	0.310	1.310	0.034	0.005
Mgs	0.626	1.626	0.021	0.003
TRJlr	10.000	11.000	0.002	0.000
Klsol	0.000	1.000	0.002	0.000
JKbl	0.000	1.000	0.002	0.000
Kur	0.000	1.000	0.002	0.000
OMas	0.000	1.000	0.002	0.000
Mmn	0.000	1.000	0.002	0.000

867

868